Université de Montréal

The implication of GPP130 shedding by PC7 and Furin in lung cancer progression

by

Priyanka Prabhala

Department of Molecular Biology

Faculty of Medicine

Thesis work carried out with the supervision of

Dr. Nabil Georges Seidah,

in partial fulfillment of the requirements of the Master of Science degree in Molecular Biology.

August 2023

Résumé

Le cancer du poumon est la principale cause de mortalité par cancer au Canada et entraîne un taux de mortalité important chez les patients. En effet, l'Organisation Mondiale de la Santé (OMS) indique que le cancer du poumon est la principale cause de décès liés au cancer dans le monde, avec 2.21 millions de diagnostics par année qui conduisent en moyenne à 1.8 millions de décès par an. Initialement asymptomatique, ce cancer évolue rapidement, devenant très invasif et métastatique, et est alors responsable de plus de morts par an que ces quatre cancers meurtriers combinés : côlon, sein, prostate et pancréas.

Les Proprotéines Convertases (PCs) sont une famille de 9 sérines protéases qui jouent un rôle dans la maturation des précurseurs de protéines. Les PCs activent/désactivent ces précurseurs en les clivant à un unique ou une paire de résidus d'acides aminés et sont ainsi essentiels pour divers processus biologiques, tels que l'activation de facteurs de croissance qui jouent un rôle vital dans la transformation cellulaire et les risques de formation de tumeurs. Parmi les neufs membres des sérines protéases identifiées, les rôles physiologiques du septième membre de la famille, PC7, restent encore largement méconnus à ce jour. Afin d'identifier davantage de substrats de PC7, un criblage protéomique quantitatif a été réalisé pour l'enrichissement sélectif de polypeptides N-glycosylés, sécrétés par les cellules hépatiques HuH7. Deux protéines transmembranaires de type II clivées par PC7/Furine, et sécrétées sous forme soluble, ont alors été identifiées : CAncer Susceptibility Candidate 4 (CASC4) and Golgi PhosphoProtein de 130 kDa (GPP130). Des études ultérieures menées sur CASC4 par

notre laboratoire ont mis en évidence son rôle protecteur contre la migration et l'invasion du Cancer du Sein Triple Négatif.

GPP130 est une protéine transmembranaire de type II avec un domaine luminal contenant des déterminants endosomaux et de récupération du Golgi, lui offrant une voie de trafic cellulaire unique. Jusqu'à présent, le rôle de GPP130 a principalement été étudié dans la liaison et le trafic rétrograde des Shiga-toxines. Un récent rapport a cependant aussi montré son implication dans la progression du cycle cellulaire et dans la prolifération des cellules du cancer de la tête et du cou. Ainsi, notre analyse du cBioPortal pour Cancer Genomics a révélé que GPP130 est amplifié jusqu'à 35% chez les patients atteints de cancer du poumon. Le travail présenté ici montre les implications du clivage de GPP130 par PC7 et Furine dans la progression du cancer du poumon, en identifiant la région de GPP130 responsable de la croissance cellulaire. Ce projet dévoile ainsi des stratégies thérapeutiques potentielles ciblant la prolifération cellulaire induite par GPP130.

Mots-clés: Proprotéine Convertases, Proprotéine Convertase 7 (PC7), Protéolyse, Cancer du poumon, GPP130, Modifications post-traductionnelles.

Abstract

Lung Cancer is the leading cause of cancer death in Canada and causes significant morbidity in patients. Globally, World Health Organization (WHO) reports lung cancer as the leading cause of cancer-related deaths, with 2.21 million diagnoses/year, resulting in approximately 1.8 million deaths/year. Initially asymptomatic, it progresses to a highly invasive and quickly metastasizing cancer. It is responsible for more deaths per year than the combined death of the four deadly cancers: colon, breast, prostate, and pancreas.

Proprotein Convertases (PCs) are a family of nine serine proteases that play a role in the maturation of secretory precursor proteins. Basic amino acid-specific PCs activate/inactivate precursor proteins by cleaving them at single or paired basic amino-acid residues. They are crucial for various biological processes, including the activation of growth factors that play a vital role in cellular transformation and the likelihood of tumor formation. Of the nine serine proteases identified, the physiological functions of the seventh member of the family, PC7, currently remain mostly unidentified. To further identify novel PC7 substrates, a quantitative proteomics screen for selective enrichment of N-glycosylated polypeptides, secreted from hepatic HuH7 cells, was performed. This identified two type-II transmembrane proteins, which were shed into soluble secreted forms by PC7/Furin: **CAncer S**usceptibility **C**andidate **4** (CASC4) and **G**olgi **P**hospho**P**rotein of **130** kDa (GPP130). Subsequent studies on CASC4 by our laboratory reported the protective role that CASC4 plays against migration and invasion in Triple Negative Breast Cancer.

GPP130 is a type-II transmembrane protein with a luminal domain containing endosomal and Golgi-retrieval determinants enabling a unique subcellular trafficking route. So far, the role of GPP130 has only been extensively studied in the binding and retrograde trafficking of Shiga toxin. However, recent reports have shown its implication in cell-cycle progression and cellular proliferation of head and neck cancer cells. Our analysis from cBioPortal for Cancer Genomics revealed that GPP130 is amplified in up to 35% of patients with lung cancer. The work presented here shows the implications of shedding GPP130 by PC7 and Furin in lung cancer progression by identifying the region of GPP130 responsible for cellular growth and unravelling potential therapeutic strategies for GPP130-induced cellular proliferation.

Keywords: Proprotein Convertases, Proprotein Convertase 7, Proteolysis, Lung Cancer, GPP130, Post-Translational Modifications

Table of Contents

List of Tables

List Of Figures

List Of Abbreviations

AA: Amino Acid
APOA-V: Apolipoprotein A-V
APT: Acyl Protein Transferase
ATP: Adenosine Tri-Phosphate

Ca^{2+}: Calcium
CASC4: Cancer Susceptibility Candidate 4
CDK1: Cyclin-Dependent Kinase 1
CDK2: Cyclin-Dependent Kinase 2
CDK4/6: Cyclin-Dependent Kinase 4 and 6
CDK6: Cyclin-Dependent Kinase 6
CMK: Chloromethylketone
cDNA: Complementary Deoxyribonucleic Acis

D6R: Hexa-D-arginine
DNA: Deoxyribonucleic Acid

EGFR: Epidermal Growth Factor Receptor
ER: Endoplasmic Reticulum
EV: Empty Vector

FL: Full Length

GB3: Globotriaosylceramide
GOLIM4: Golgi Integral Membrane protein 4
GPP130: Golgi Phosphoprotein of 130kDa

HDAC: Histone Deacetylases

LDLR: Low-Density Lipoprotein Receptor

mAb: Monoclonal antibody
MDM2: Murine Double Minute 2
MHC 1: Major Histocompatibility Complex 1
MVB: Multi-Vesicular Bodies

NK Cells: Natural Killer cells
NMT: N-Methyltransferase
NSCLC: Non-Small Cell Lung Cancer
NSCLC-NOC: Non-Small Cell Lung Cancer – Not Otherwise Specified
NTD: N-terminal Domain

PACE4: Paired basic Amino acid Cleaving Enzyme 4
PAT: Protein Palmitoyltransferase
PC: Proprotein Convertase
PC1: Proprotein Convertase 1
PC2: Proprotein Convertase 2
PC4: Proprotein Convertase 4
PC5: Proprotein Convertase 5
PC7: Proprotein Convertase 7
PCSK9: Proprotein Convertase Subtilisin Kexin 9
PTM: Post Translational Modifications

QPCR: Quantitative Polymerase Chain Reaction

RVKR-CMK: Decanoyl-Arg-Val-Lys-Arg Chloromethylketone
RT-PCR: Real-Time Polymerase Chain Reaction

SAC: Spindle Assembly Checkpoint
SCLC: Small Cell Lung Cancer
SCRIB: Scribbled homolog protein
SKI-1: Subtilisin kexin isoenzyme-1/
SOCE: Store Operated Calcium Entry
SOL.: Soluble
STEC: Shiga Toxin producing Escherichia Coli
STIM1: Stromal Interaction Molecule 1
STX: Shiga Toxin

TGN: Trans Golgi Network
TM: Transmembrane
TP53: Tumor Protein 53

VEGF: Vascular Endothelial Growth Factor

WHO: World Health Organisation
WT: Wildtype

Acknowledgements

First and foremost, I would like to thank my supervisor, Dr. Nabil Georges Seidah, for giving me an opportunity to work in his laboratory when I had lost all hope in fulfilling my dream of having a career in science. I find it hard to believe that I was able to write and complete this thesis, which, needless to mention, would not have been possible without Dr. Seidah's continuous guidance, constant support and his never-ending enthusiasm for science that kept me motivated throughout.

I am also extremely grateful to Dr. Annik Prat, Alexandra Evagelidis, Ann Chamberland, Ali Ben Ouadda, Anna Roubtsova, Delia Resiga, Rachid Essalmani, Mailys Le Devehat, Chloé Porcheron, Sepideh Mikaeeli and Jisca Borgela. Their insightful comments and well-thought-out advice were very beneficial in the progress of this project. I would also like to thank all the past members of Seidah laboratory for their help and support, especially Stephanié Duval, without whom GPP130 would not have been identified as a PC7 substrate.

Special thanks to my partner and now my husband, Vatsal Sachan, for constantly pushing me to challenge myself and give my best in everything I do. I would not have been here without you. I love you.

I would also like to express my gratitude to Dr. Laurence Jaworski for being patient with the yearlong treatment of my Uveitis.

Lastly, needless to mention, I am thankful for my family members for motivating me when I was low and all my friends for their continuous encouragement, motivation, and support.

Chapter 1. General Introduction.

The family of proprotein convertases consists of 9 serine proteases, PC1, PC2, PC4, PC5, PACE4, PC7, Furin, SKI-1 and PCSK9, that function in the maturation /activation/inactivation of a multitude of secretory precursor proteins, viral protein processing and progression of diseases like cancer.

Given that many functions of PC7 remain obscure to date, our laboratory has generated a quantitative proteomics screen to identify potential new substrates of PC7.

Since the main objective of this thesis is to discuss the role of a Golgi-resident protein GPP130, identified as a PC7 substrate, in the progression of lung cancer, a brief introduction to the hallmarks of cancer, proprotein convertases, and GPP130 will be presented first.

1.1. Introduction to Cancer Biology

1.1.1 Cell-division cycle; a major factor governing cancer proliferation

Cells are the basic structural and functional unit of life that make up all living organisms. In the event of cell death or damage to cells, or when the body requires new cells, cells are able to grow and divide, generating new daughter cells that replace the dead or damaged ones. This process occurs through a carefully controlled process termed ‘Cell Division’ where one cell divides into two, two cells divide into four, four cells divide into eight and so on. In the human body, there are two types of cell division: Mitosis and Meiosis. Mitosis is the vegetative replication of cells, where the daughter cell is the exact replica of a parent cell. Meiosis is the cell division that produces four haploid cells instead

of precise duplicates of the parent cell, which is required to produce sperm or egg cells [1, 2].

This mitotic cell cycle consists of two main phases: Interphase (G0, G1, S G2 phases) and M phase (Mitotic phase) (Figure 1) [3].

The sub-stages of interphase consist of the following sub-stages:

- **G0 (Gap 0) Phase**: This is the resting phase, where the cell neither divides nor prepares itself for cell division.
- **G1 (Gap 1) Phase**: The cell doubles in size and synthesizes mRNA and proteins required for DNA synthesis.
- **S (Synthesis) Phase**: At this stage, the cellular DNA replicates itself generating two copies of the entire genome. With the help of histone proteins, the loose DNA condenses into chromatids, subsequently organizing themselves into X-shaped chromosomes. Each chromosome consists of two chromatids.
- **G2 (Gap 2) Phase:** The cell prepares itself for the next stage by preparing the final molecules, such as microtubules necessary for spindle formation required during mitosis.

And finally, the **Mitotic stage (M stage)** consists of the following sub-stages:

Prophase, **Prometaphase**, **Metaphase**, **Anaphase**, and **Telophase** (Figure 1).

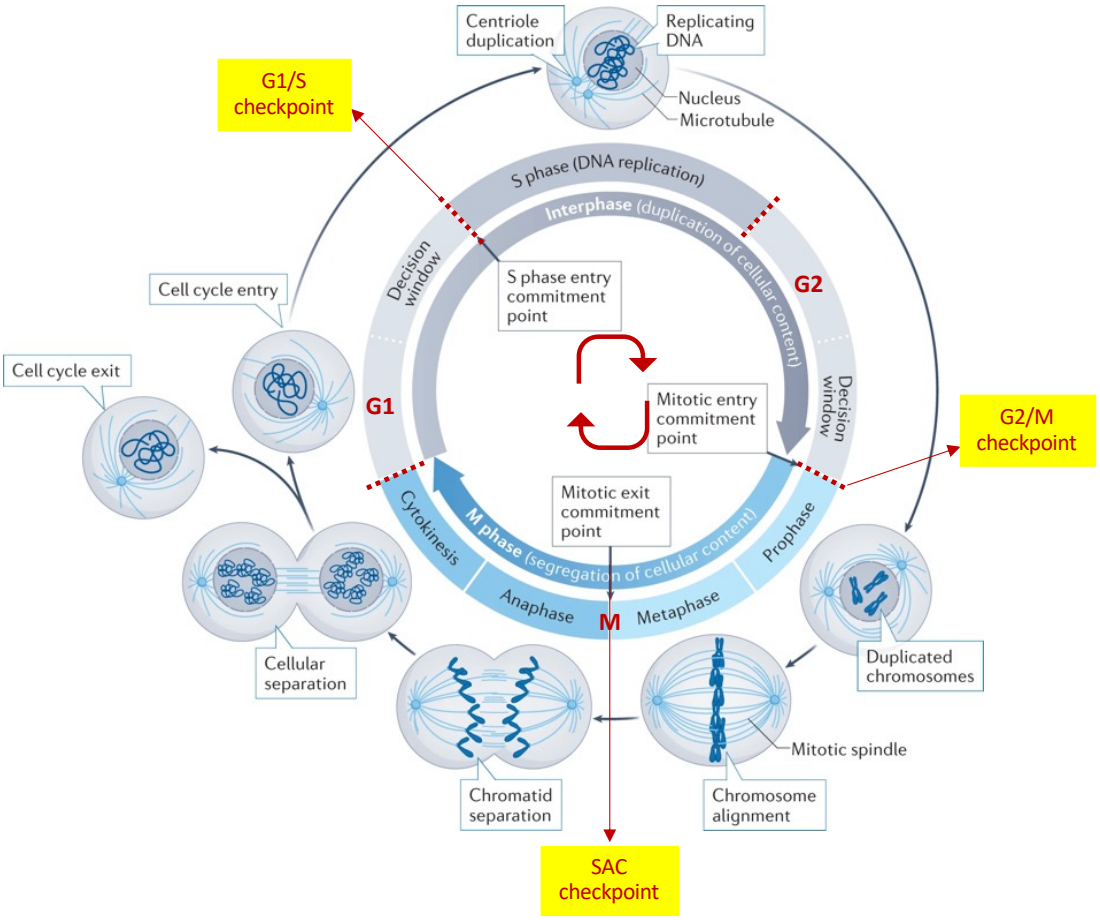

Figure 1: Eukaryotic Cell-Division Cycle

Figure 1: The eukaryotic cell cycle involves the duplication of cellular content in interphase, followed by division in the M phase to generate two identical cells. The cell cycle consists of distinct events, namely DNA replication and the segregation of replicated DNA, which occur at different stages. DNA replication occurs during the specific interphase phase known as the "S phase," while DNA segregation occurs during mitosis (M phase). Cytokinesis, which happens at the end of the M phase, facilitates the separation of cellular content and marks the completion of a cell cycle. After completing a cell cycle, a cell can exit the cycle or enter a new round of cell division. The progression of the cell cycle during interphase is regulated both before and after the S phase. The decision to initiate a new cell cycle, explicitly entering the S phase, is made within a defined window preceding the S phase. Similarly, following the S phase, there is a decision window during which a cell can commit to entering mitosis. The commitment to exit mitosis occurs at the metaphase-anaphase transition during the M phase. Figure adapted from Matthews et al. 2022. [4]

The progression of the cell-division cycle is closely modulated by Cyclin-Dependent Kinases (CDKs) and their subunits. CDKs (CDK1, CDK2, CDK4/6), which are serine/threonine kinases that are activated when they bind to their cyclin partner. They also act as cell-cycle checkpoints that have been evolutionarily conserved to ensure the generation of two genetically identical daughter cells. The expression of these cyclin partners rises and drops throughout the cell cycle, so each CDK is transitorily activated. These checkpoints function as DNA surveillance procedures and prevent the accumulation and multiplication of errors in DNA duplication. These checkpoints slow down the cell division cycle to ensure the errors in DNA replication are repaired, halting cells from progressing to the next stage of cell division. In case of irreparable damage to the DNA, the checkpoints induce exit from the cell cycle or even cause cell death, thus preventing the production of cells with genetic errors [4]. There are three crucial checkpoints: the G1/S checkpoint, the G2/M checkpoint, and SAC (Spindle Assembly Checkpoint) [5]. In the G1/S checkpoint, CyclinD-CDK4/6 and CyclinE-CDK2 successively phosphorylate Rb (Retinoblastoma), thereby disassociating the HDAC repressor complex, allowing transcription of genes required for DNA replication that occurs in the S phase. The G2/M checkpoint occurs after DNA has been replicated in the G2 phase, and the activity of CyclinB-CDK1 in this checkpoint prevents the cell from entering the M phase if DNA is damaged. Finally, the SAC checkpoint ensures the attachment of spindle microtubules to kinetochores by sensing the area occupied by the microtubules on the kinetochore surface. Kinetochores are a group of large proteins that connect microtubules to chromosomes, and their function is to provide an optimal distribution of replicated DNA into daughter cells so each daughter cell has an identical copy of DNA. [6] It is believed that SAC also estimates the accumulation of tension

between all the inter-kinetochores when one-half of kinetochores (sister kinetochores) get linked to opposite spindle poles for the generation of two daughter cells [7].

Dysregulation of the tightly regulated process of cell division causes dividing cells to accumulate genetic errors and proceed into the cell cycle, giving rise to the proliferation of aneuploid or polyploid daughter cells. These cells may proliferate further, generating a cluster of aneuploid cells that are able to evade death signals giving rise to diseases such as cancer, causing uncontrolled proliferation of abnormal cells in the body [8, 9].

Chapter 1.1.2 – Hallmarks of Cancer

The development of cancer is a multi-step process during which cells, over time, accumulate multiple genetic mutations leading to uncontrollable division, growth of abnormal cells, and evasion of cell death. Usually, the genetic alterations occur in at least two pronounced categories of genes; proto-oncogenes and tumour suppressors. Proto-oncogenes are genes responsible for controlling cell growth and cell division. When mutated, a proto-oncogene is activated quantitatively or qualitatively, promoting tumor growth. Contrary to proto-oncogenes, tumour suppressor genes, in operational conditions, suppress the growth of tumours. When inactivated, tumour suppression is lost, and these genes positively regulate tumor growth [10].

In the year 2000, the concept of ‘Hallmarks of Cancer’ was proposed by Hanahan and Weinberg to distinguish the various complexities of cancer phenotypes and genotypes based on the manifestation of six pivotal alterations in cell physiology that can collectively drive malignant growth [8].

The six hallmarks identified that cancer cells acquire (Figure 2) in the multi-step process of tumorigenesis consisted of the following:

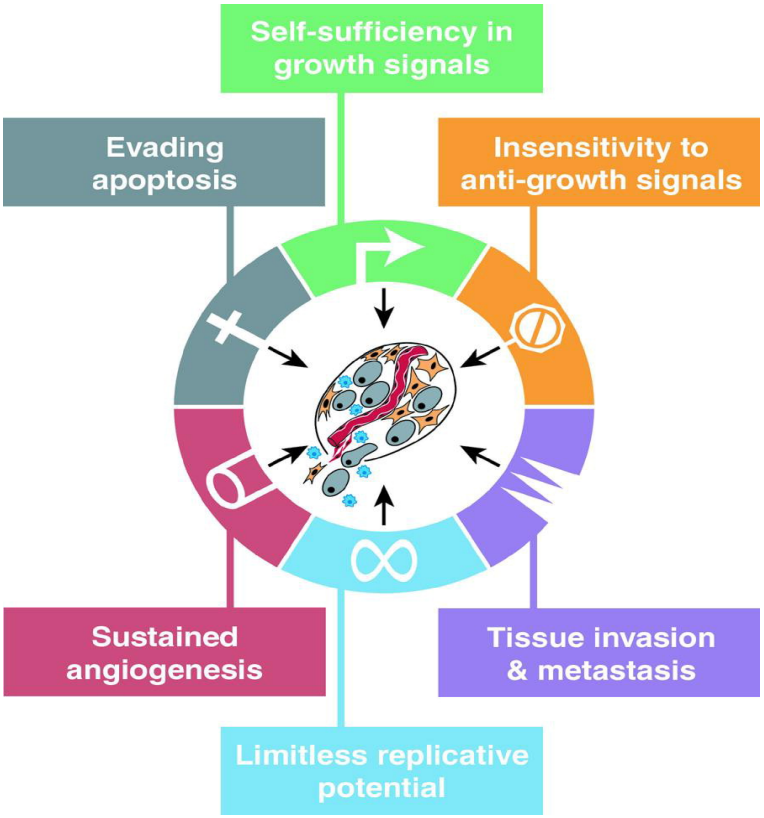

Figure 2: Hallmarks of Cancer, circa 2000

Figure 2: The six hallmarks of cancer formulated initially in 2000. Figure adapted from Hanahan, Cell 2000 [8].

(i) Sustenance of proliferation: For a normal cell to move from a quiescent state to a state of active proliferation, there is a requirement for mitotic growth signals. Growth signals are relayed into the cell when transmembrane receptors bind to signalling molecules like diffusible growth factors or components of the Extracellular Matrix. However, in stark contrast, tumour cells show a significant lack of dependence on

exogenous growth signals. Many cancer cells attain the ability to synthesize their own growth factors to proliferate, creating a positive feedback loop [8, 11, 12].

(ii) Evasion of growth suppressors: For proper tissue homeostasis, it's essential that there are signals in place to prevent excessive cell proliferation. These signals work similarly to how growth factors are transmitted through cell surface receptors. These growth-inhibiting signals enter the cell and connect with internal signaling pathways that ultimately hinder further growth. In the case of cancer cells, they manage to bypass these signals that restrict proliferation, allowing them to persistently replicate [8, 13].

(iii) Resistance to cell death (apoptosis): Cancer cells commonly evade apoptosis by mutations in the p53 tumour suppressor gene resulting in functionally inactive p53 protein. p53 protein, a crucial component of the DNA damage response, is responsible for inducing apoptotic effector cascade in normal cells [8, 14].

(iv) Ability to replicate immortally: Most mammalian cells have an intrinsic cell-autonomous mechanism to control their cell -division. This is disrupted in cancer cells, in addition to evasion of growth suppressors and cell death, causing them to acquire a limitless replicative potential. Additionally, the telomerase enzyme and its maintenance play an important role in cancer cells' ability to develop the ability to replicate immortally [8, 15].

(v) Sustained angiogenesis: Angiogenesis is a carefully regulated process by which new blood vessels form from the existing vasculature to provide oxygen and nutrients to support the growth of bodily tissues and cells. One way tumors continue growing is by

activating angiogenesis by changing the balance of angiogenic inducers and inhibitors by altering gene transcription [8].

(vi) Activation of invasion and metastasis: Invasion and Metastasis, though closely allied, are complex mechanisms that remain less understood to date, albeit both processes involve alterations in the physical coupling of cells to their microenvironment. However, a widely observed alteration involves loss of E-Cadherin function, which suppresses invasion and metastasis [8, 16].

By 2011, extensive studies on cancer biology resulted in the addition of two more hallmarks and two enabling characteristics to the list (Figure 3);

(i) Avoiding immune system destruction: To illustrate the ability of tumour cells to evade recognition and destruction by the immune system, Teng et al. performed a study on immunocompromised mice with carcinogen-induced tumours. They revealed that in the absence of T cells and NK (Natural Killer) cells, the tumours in mice grow more rapidly [17].

(ii) Reprogramming of cellular metabolism: It is known that normal cells rely on oxygen uptake to metabolize glucose and produce energy through a regulated process known as glycolysis. In contrast, to promote an increase in cell proliferation, tumour cells reprogram cellular metabolism and increase their rate of glucose uptake to efficiently synthesize ATP and lactate production, a process known as the Warburg effect [18].

(iii) Tumour-promoting inflammation: Inflammatory responses can play critical roles during the development of tumours. These responses are pivotal in tumour initiation, invasion and metastasis. Inflammation contributes to these processes by providing the

tumour microenvironment with growth factors that help in sustained proliferative signalling and evasion of cell death of tumour cells [19].

(iv) Genetic instability and/or mutations: As aforementioned, cancer development is a multi-step process in which cells have, over time, acquired multiple oncogenic mutations. The acquisition of genomic mutations confers a growth advantage to the cells, enabling them to outgrow in a local tissue environment. In addition to heritable genomic mutations, mutations may also arise due to epigenetic changes like DNA methylation and/or histone modifications, subsequently affecting the regulation of gene expression [20].

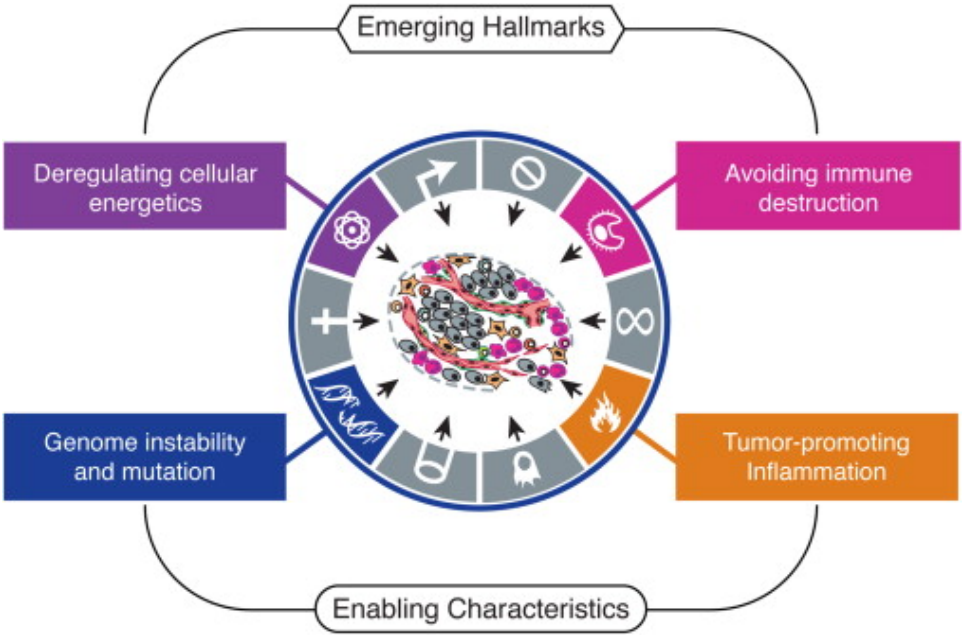

Figure 3: Hallmarks of Cancer, circa 2011

Figure 3: By 2011, a growing body of research indicated that two additional characteristics, referred to as emerging hallmarks, played a role in the development of various types of cancer. One hallmark involved the ability of cancer cells to modify or reprogram cellular metabolism to support their uncontrolled growth efficiently. The second hallmark enabled cancer cells to evade the immune system's attempts to destroy them. In 2011, they were recognized as emerging hallmarks due to their increasing importance in cancer research. Furthermore, the acquisition of both core and emerging

hallmarks was facilitated by the characteristics of cancer, which promoted genomic instability and its ability to acquire genetic mutations. Additionally, inflammation caused by the activation of innate immune cells can inadvertently support multiple hallmark capabilities, suggesting these two qualities must be listed as the 'enabling characteristics' in cancer progression. This figure was adapted from [Hanahan, Cell, 2011] [21]

The eight hallmarks, laid out in 2011, as a refinement to the cancer hallmarks model raised the question, 'Is there a need to add more hallmarks that can apply to a broader subset of human cancers?'

In 2022, Hanahan further proposed two emerging characteristics and two prospective new hallmarks that could eventually be embodied as the core components of the cancer hallmarks model based on a growing body of evidence, as below:

(i) Unlocking phenotypic plasticity: Tumour cells sustain various molecular and physical changes, termed 'cellular plasticity,' in response to many factors ranging from the microenvironment to epigenetic alterations during cancer progression. Recent studies show these changes are widespread as the tumour progresses. It is essential to understand the molecular mechanisms underlying different forms of cellular plasticity to treat cancer better, thus making this an acquired hallmark of cancer cells.

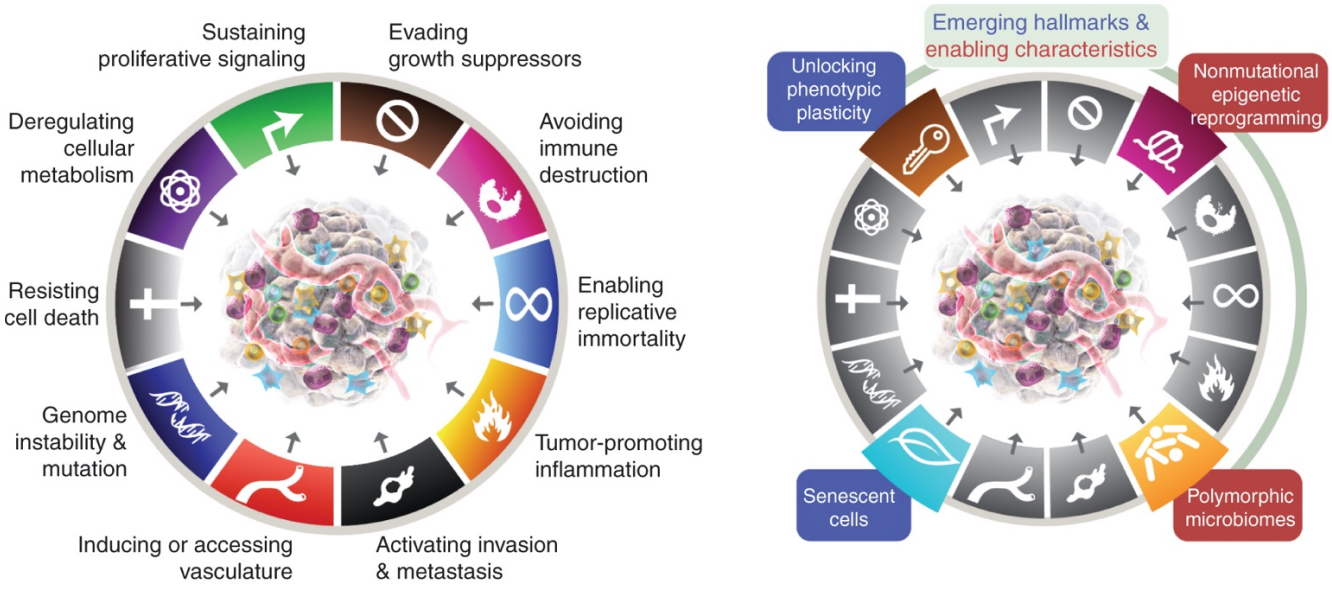

Figure 4: Hallmarks of Cancer, circa 2022

Figure 4: (LEFT) The Hallmarks of Cancer, as of 2022, embodied eight hallmark capabilities and two enabling characteristics. (RIGHT) Given the growing body of evidence, Hanahan and Weinberg proposed new emerging hallmarks and enabling characteristics and proposed the addition of a) unlocking phenotypic plasticity, b) non-mutational epigenetic reprogramming, c) polymorphic microbiomes, and d) senescent cells to the list. This illustration was adapted from Hanahan, *Cancer Discovery*, 2022 [22].

(ii) Non-mutational epigenetic reprogramming: One of the most common features established in various cancers is the global variation in their epigenetic landscape. Cancer cells reprogram a multitude of gene-regulation systems to modify the expression of genes to eventually acquire capabilities of the aforementioned cancer hallmarks.

(iii) Polymorphic microbes: It is well established that the trillions of microbes that inhabit a human body aid in the digestion of food. However, recent studies have shown some of these microbes also play a crucial role in influencing the risk of cancer. Additionally, tumour cells and microbes coevolve and help in each other's survival and replication, suggesting that microbial cells can be vital in tumour initiation and progression [23].

(iv) Senescent cells: Previously, Hanahan discussed senescence as a potential barrier against cancer without dismissal of the possibility that it may be an artifact of cell culture without representing an actual cell phenotype in vivo. The significance of senescent cells as crucial elements in the tumor microenvironment were acknowledged as part of the emerging hallmarks in 2022. Currently, the role of cellular senescence in maintaining tissue balance and its connection to cancer is widely accepted. Various important morphological and metabolic characteristics associated with senescence have also been uncovered. Research has demonstrated that senescent cells can even promote tumor development and the progression of malignancy in specific situations. As a result, Hanahan proposed the inclusion of senescent cells as a significant component within the tumor microenvironment, suggesting incorporating it in the renewed hallmarks of cancer [22].

The next section of this thesis will briefly summarize the different types of lung cancer, their causes and the current therapeutic strategies given to patients.

Chapter 1.1.3 Lung Cancer

In Canada, lung Cancer is the leading cause of cancer death and causes significant morbidity in patients [24]. According to a report by the World Health Organization, lung cancer is the leading cause of cancer-related deaths worldwide [25]. Every year around 1.8 million people are diagnosed with lung cancer, and 1·6 million die due to the disease [26]. Initially asymptomatic, it progresses to a highly invasive and quickly metastasizing cancer. It is responsible for more deaths per year than the combined death of the four deadly cancers: colon, breast, prostate, and pancreas. For to this reason, patients are already at stage 3 or 4 of cancer when presented to the clinic. About 90% of the cases

result from smoking and tobacco product usage. Additionally, other factors such as genetic inheritance, air pollution, exposure to asbestos and chronic infections can also give rise to lung carcinogenesis [27]. Patients who present with this disease are usually above 50 years of age, and men are more susceptible to it than women.

Since lung cancer has the ability to originate from any/multiple sites on the bronchial tree, it is considered a highly heterogenous carcinoma with patients having varying symptoms. Lung Cancer is broadly categorized into two different sub-types, mentioned below, depending on how they grow and spread:

(i) Small Cell Lung Carcinomas (SCLC): Further categorized into Oat Cell Cancer and Combined Small Cell Carcinoma, SCLCs originate in lung hormonal cells with the growth of dedifferentiated cells and encompass the lung mediastinum resulting in central mediastinal tumors. These types of cancers are extremely aggressive and comprise about 15% of all lung cancers. They are able to rapidly spread to lymphatic vessels and lymph nodes.

(ii) Non-Small Cell Lung Carcinoma (NSCLC): NSCLCs are categorized into adenocarcinoma, squamous cell carcinoma and large cell anaplastic carcinoma, also referred to as Non-Small Cell Lung Carcinoma Not Otherwise Specified (NSCLC-NOC). Starting in the peripheral lung tissue, adenocarcinomas arise in the epithelial cells of segmental bronchi. On the contrary, squamous cell lung carcinomas arise in epithelial cells of the main and lobar bronchi. However, large cell carcinomas are more centrally located and invade the lung mediastinum and its structures. NSCLC-NOC cancers particularly behave as small-cell lung cancers in that they are able to spread rapidly and prove to be very fatal [27].

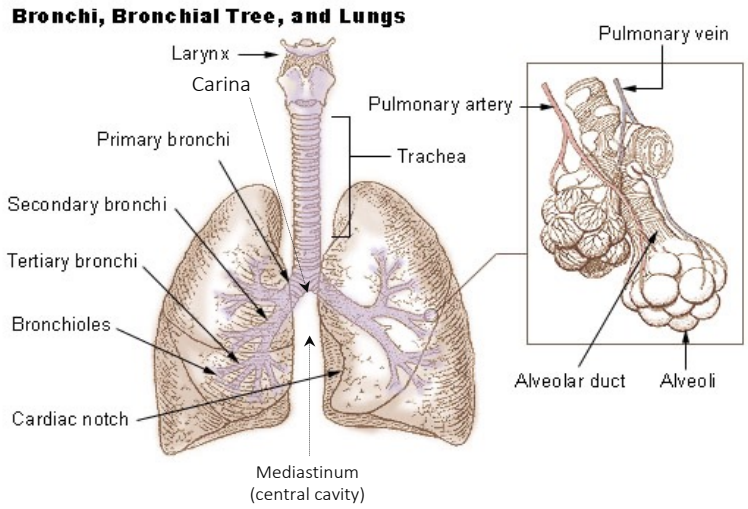

Figure 5: Anatomy of the lung

This categorization helps predict the patient's treatment regimen and determines their subsequent prognosis [28].

Lung Cancer (LC) Type	% of all LC incidents	Anatomic Location
Squamous cell lung cancer (SQCLC)	25 – 30%	Arise in main bronchial tree and advance into carina
Large Cell Anaplastic Carcinomas (LCAC) / NSCLC-SOC	10%	Tumors lack the classic glandular or squamous morphology
Adenocarcinomas	40%	Arise in peripheral bronchi
Small Cell Lung Cancers (SCLC)	10 – 15%	Derive from hormonal cells, disseminate into submucosal lymphatic vessels and regional lymph nodes, NO bronchial invasion.

Table 1: Different types of lung cancer and their anatomic location

The current therapeutic strategies for lung cancer treatment may include various treatments like chemotherapy, radiotherapy, targeted therapy (precision medicine), immunotherapy, hypothermia, hormone therapy and/or surgery. However, despite the development of these intensive therapies, the survival rate for lung cancer still remains bleak. Further research is needed to recognize additional genetic changes that may affect the patient's clinical outcome, and detecting cancer early will help patients' survival in the long run. Needless to say, prevention is better than cure, and a very crucial criterion for the prevention of this disease is to quit/reduce smoking and the use of tobacco products [27].

Chapter 1.2 – Post-translational Modifications of Secretory Proteins

Post-translational modifications (PTMs) play a crucial role in the functioning of all organisms. PTMs refer to reversible or non-reversible modifications of proteins that occur after translation, catalyzed by various essential enzymes [29, 30]. Despite the human genome comprising approximately 22,000 genes, the reported number of proteins exceeds 10 million. This highlights the significance of alternative splicing, alternative promoters and mRNA editing (resulting in ~200,000 mRNA transcripts), as well as PTMs (10 million proteins/peptides), in generating a wide range of functional protein diversity within cells. The latter modifications encompass diverse processes such as phosphorylation, glycosylation, acylation, ubiquitination, nitrosylation, methylation, acetylation, lipidation and proteolysis and hold importance in every aspect of biology. To date, around 200 PTMs have been identified, with proteolysis being a common irreversible modification mediated by proteases.

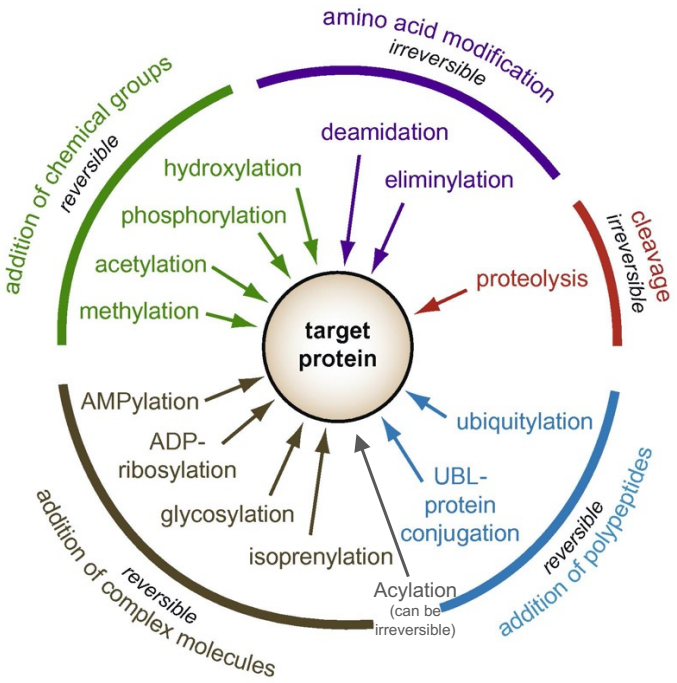

Figure 6: Diversity of Post-Translational Modifications of a target protein

Fig 6: PTMs refer to alterations made to proteins after they have been translated. These Modifications range from a) modification of the chemical structure of amino acid side chains, b) the addition of chemical groups or complex molecules to specific amino acids, c) the covalent linkage of polypeptides, d) the cleavage of the peptide bond between two amino acids, termed proteolysis. Figure adapted from Ribet, *FEBS Letters*, 2010. [31]

To better understand the subsequent work in this thesis, it is essential to understand the consequences of Palmitoylation and Myristoylation, two types of Acylation of a target protein.

Palmitoylation: This PTM involves the covalent attachment of palmitic acid to either cysteine (S-palmitoylation), serine or threonine (O-palmitoylation), usually to the cytosolic tail of membrane proteins. Generally, the hydrophobicity of a protein is enhanced upon its palmitoylation resulting in better membrane association. Additionally, the cell employs this PTM to alter the cellular localization of the target protein [32].

Myristoylation: This is a type of lipidation modification wherein Myristic acid, a 14-carbon saturated fatty acid, is covalently attached to a Glycine residue at the N-terminus of the

cytosolic tail of type_II transmembrane target proteins by N-MyristoylTransferase (NMT). This PTM plays a crucial role in membrane targeting, protein-protein interactions and various cell signalling pathways [32].

Palmitoylation and Myristoylation are the two common lipidations strongly linked to the initiation and progression of cancers and the modulation of cancer metabolism [32].

The most prevalent irreversible PTM is by proteolysis performed by specific proteases. These enzymes cleave proproteins at particular locations, yielding multiple products. Proteolysis plays a significant role in generating bioactive forms of proteins or inactivating them. The major classes of proteases encompass five categories: metallo, aspartyl, cysteine, serine, and threonine proteases [33].

Chapter 1.2.1 Proprotein Convertases (PCs)

Many secretory proteins are initially synthesized as precursors proteins which are later cleaved at specific sites by Proprotein Convertases (PCs) to subsequently generate mature proteins [34]. The biology of Proprotein Convertases is essential to understand in the context of tumor progression since a majority of these inactive precursor proteins are growth factors, adhesion molecules and matrix metalloproteases that, once activated, play a crucial role in cellular transformation and acquisition of tumorigenic phenotypes [35, 36].

Secretory mammalian proprotein convertases are a family of nine serine proteases (figure 7) that are related to bacterial subtilisin and yeast kexin, present in the secretory pathway of the cell, i.e., endoplasmic reticulum, Golgi, cell surface, endosomes and

extracellular milieu. Among them, seven, namely, PC1 (**Proprotein** **C**onvertase 1), PC2, PC4, PC5, PC7, PACE4 (**P**aired basic **A**mino **C**leaving **E**nzyme 4) and Furin, cleave (↓) cellular or pathogenic precursor proteins at single or paired basic amino acid (aa) residues within the motif (R/K)-(2X)n-(R/K)↓, where n = 0, 1, 2, or 3 spacer aa, and X is a variable aa, resulting in their activation or inactivation [34, 37]. In contrast to the above seven PCs, the eighth member of the mammalian PC family, namely, SKI-1 (**S**ubtilisin **K**exin **I**sozyme 1), cleaves its substrates at non-basic residues at the C-terminal end of the motif R-X-(L/V/I)-X↓, where X is any amino acid except Proline and Cysteine. The last member, PCSK9 (**Proprotein** **C**onvertase **S**ubtilisin **K**exin 9), only cleaves itself at its internal sequence motif (V/I/L)-FAQ↓, after which it loses its protease activity as it remains non-covalently complexed to its inhibitory prodomain and thereafter functions as a binding protein to specific receptors present on the cell surface. Particularly, PCSK9 amplifies the endosomal and lysosomal degradation of LDLR (Low-Density Lipoprotein Receptor) that is implicated in cholesterol regulation and lipid homeostasis [34].

Proprotein Convertases play a role in the activation or inactivation of polypeptide hormones, growth factors and their subsequent receptors and help in the progression of diseases like cancer. In addition, Furin and SKI-1 are also implicated in the processing of viral proteins and regulating virus cell entry into the body [37, 38].

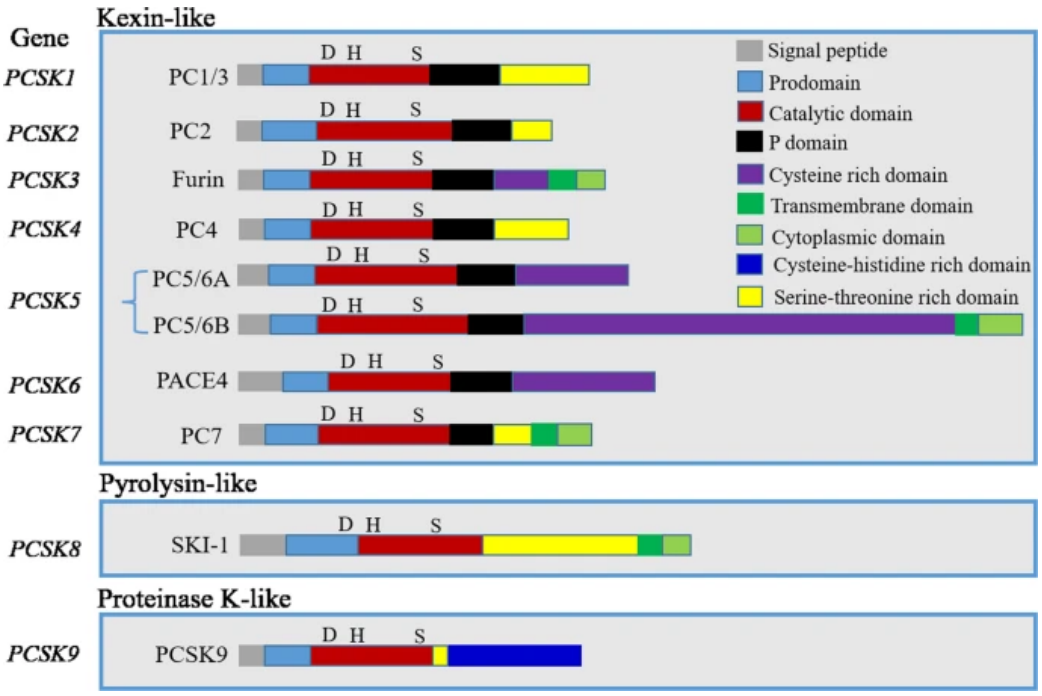

Figure 7: Structure of the nine identified Proprotein Convertases

Fig 7: This diagram depicts the structural template of all the proprotein convertases identified to date and highlights their various structural domains. The residues D (Aspartate), H (Histidine), and S (Serine) within the catalytic domain of each proprotein convertase are specifically marked since these represent the active site residues within the domain. Illustration adapted from He, *Oncogene*, 2022 [36].

It is important to delve into PC7 specifically since this work focuses on its implication in the shedding of GPP130.

Chapter 1.2.2. Proprotein Convertase 7 (PC7)

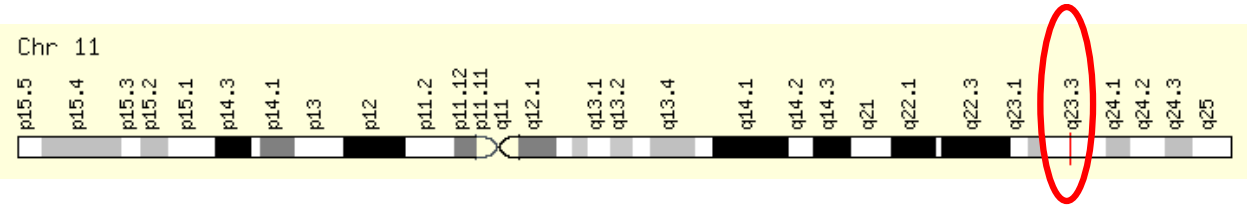

Figure 8: Chromosomal location of *PCSK7*

Fig 8: This illustration shows the chromosomal location of the *PCSK7* gene. The gene is located on chromosome 11, position q23.3. This illustration was taken from ENSEMBL.

The ubiquitously expressed human *PSCK7* gene is located on chromosome 11q23.3 and encodes a secretory type I membrane-bound protease, PC7, synthesized in the Endoplasmic Reticulum (ER). It is initially synthesized as a ~102kDa proPC7 zymogen and subsequently undergoes autocatalytic cleavage to produce a ~92kDa inactive mature PC7 [39]. This protease cleaves precursor proteins at single/paired basic amino acid residues at the sequence **(R/K)X_n(R/K)** ↓ where n = 0, 1, 2, or 3 spacer aa, and X is a variable aa. The only known specific substrate of PC7 identified so far is the shedding of the type_II transmembrane human Transferrin Receptor 1 (hTfR1) [40, 41]. In mice lacking *Pcsk7,* it was reported to partially process proBrain Derived Neurotrophic Factor (proBDNF), partly explaining the anxiolytic phenotype observed in these mice (PMID: 24101515).

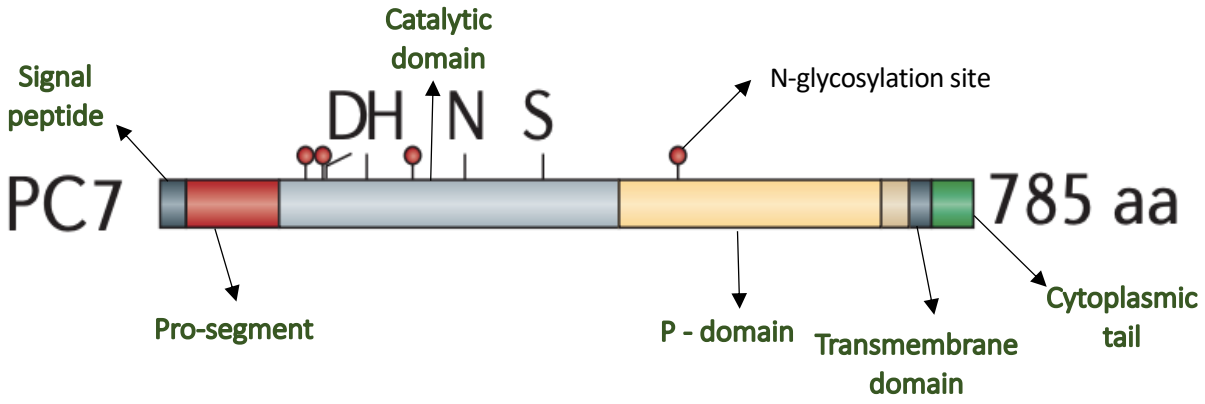

Figure 9: Structural template of Proprotein Convertase 7

Fig 9: This diagram depicts the structural template of proprotein convertase 7. The residues D (Aspartate), H (Histidine), and S (Serine) within its catalytic domain are specifically marked since these represent the active site residues within this domain. Illustration adapted from Seidah, *Nature Reviews Drug Discovery*, 2012 [37]

PC7 was recently shown to regulate lipoprotein metabolism in a non-enzymatic fashion by modulating the levels of circulating ApoA-V [42].

Of the nine serine proteases identified, the physiological roles of the seventh member of the family, PC7, currently remain mostly unidentified. To further identify novel PC7 substrates, a quantitative proteomics screen for selective enrichment of N-glycosylated polypeptides, secreted from hepatic HuH7 cells, was performed. The screen identified two type-II transmembrane proteins, shed into soluble secreted forms by PC7/Furin: CASC4 and GPP130 [43]. Further on in the thesis, the available literature on GPP130 will be summarized.

Chapter 1.2.3 Implication of Proprotein Convertases in Cancer

Several studies have demonstrated the novel roles of PCs in various cancers like head and neck cancer [44], prostate cancer [45], breast cancer [46], skin, lung, colon and nervous system cancers [47], [48], [49]. For instance, Page et al. reported the increased expression of the proprotein convertase Furin at the RNA and protein levels in different human ovarian cancer cell lines. Additionally, it was noted that Furin is preferentially expressed in ovarian tumors with poor prognosis, suggesting Furin predicts decreased survival in ovarian cancer patients [48]. Similarly, some reports have also demonstrated the effect of PC silencing in the context of cancers. A study by Bassi et al. (2010) showed that the inhibition of PACE4 resulted in reduced skin cancer cell proliferation and tumor development in vivo [50]. Additionally, a study published by our own lab connected *Pcsk9* deficiency with liver metastasis of melanoma. In this study, the authors injected B16F1 melanoma cells into the spleen of either wildtype or *Pcsk9* deficient mice and followed the metastasis to the liver over twelve days. Their findings showed that *Pcsk9* deficiency in mice significantly reduced melanoma metastasis [51].

According to a recent study, inhibition of PCSK9, a protein that plays a vital role in regulating cholesterol metabolism, can enhance the response of tumors to immune checkpoint therapy. This effect occurs through a mechanism that is distinct from PCSK9's traditional role in regulating cholesterol levels. The inhibition of PCSK9, whether through genetic deletion or the use of PCSK9 antibodies, has been shown to upregulate the expression of **M**ajor **H**isto**C**ompatibility protein class **I** (MHC I) on the surface of tumor cells. This, in turn, facilitates the infiltration of cytotoxic CD8+ T cells into the tumor microenvironment. The study suggests that PCSK9 interferes with the recycling of MHC I by physically associating with it, leading to its lysosomal degradation. These findings collectively indicated that inhibition of PCSK9 holds promise as a strategy to enhance the effectiveness of immune checkpoint therapy in cancer treatment [52].

These reports show the implication of proprotein convertases in tumor progression and that targeting PCs is a potential therapeutic strategy in cancer patients.

Chapter 1.3 – GOLIM4/GPP130

Golgi Phosphoprotein of 130kDa (GPP130) is a type II cis-Golgi protein with a 20 amino-acid long cytoplasmic tail, a transmembrane domain, and a long luminal domain that consists of both Endosomal and Golgi-retrieval determinants, thus enabling a unique trafficking route for the protein.

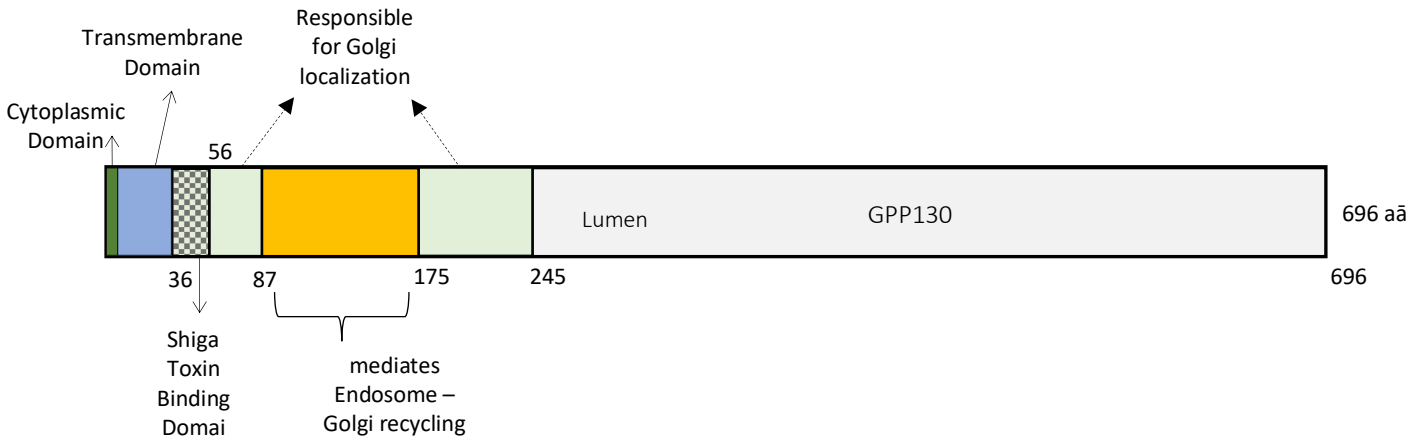

Figure 10: Structural template of GPP130

Fig 10: The diagram illustrates the structure of the GPP130 protein, demonstrating its short cytoplasmic tail, the transmembrane domain and a long luminal domain. The luminal domain consists of regions responsible for both its Golgi and Endosomal localization.

GPP130 is predominantly present in the trans-Golgi network. When the cells are treated with agents that disrupt their luminal pH, GPP130 can redistribute itself to endosomes. Upon removing its exposure to these agents, it can undergo Endosome-to-Golgi retrieval [53]. For instance, Manganese treatment induces oligomerization of GPP130 and rapidly traffics the protein to Multi-Vesicular Bodies (MVBs), with its subsequent degradation in lysosomes [54]. Further, a study by Mukhopadhyay S. et al. in 2013 revealed that Shiga-toxin, a toxin responsible for causing Shiga-Toxicosis, binds to the luminal domain of GPP130, upon which GPP130 sorts this complex to the Golgi - Endoplasmic Reticulum, where the toxin exerts its cytotoxic effects [55]. In 2010, Carnegie Mellon University Researchers discovered Manganese, an element found in nature, that can neutralize the lethal effects of Shiga toxin infections [54].

A recent study explored the association between the GPP130/GOLIM4 gene and head-and-neck cancer, specifically investigating its relationship with downstream targets of stromal interaction molecule 1 (STIM1). STIM1 is a calcium channel protein involved in the Store-operated calcium entry (SOCE) pathway, which is activated when calcium levels in the endoplasmic reticulum (ER) decrease. The study showed that GPP130 is a downstream target of STIM1 and that the STIM1-GPP130 signalling axis is crucial in the proliferation of head and neck cancers. In alignment with STIM1, there was a notable elevation in the expression of the GPP130 protein in head and neck cancer cells. Additionally, this study revealed that GPP130 plays a role in cell cycle progression and cell proliferation in head-and-neck cancer cells by influencing the expression levels of MDM2 and CDK6 [56].

In line with these observations, our laboratory analyzed the cBioPortal for Cancer Genomics Database. It showed that GPP130/*GOLIM4* is amplified in up to 35% of the patients diagnosed with lung cancer and >10% of head and neck cancer patients (figure 11).

This analysis eventually led to the subsequent work of this thesis *[manuscript in progress]*.

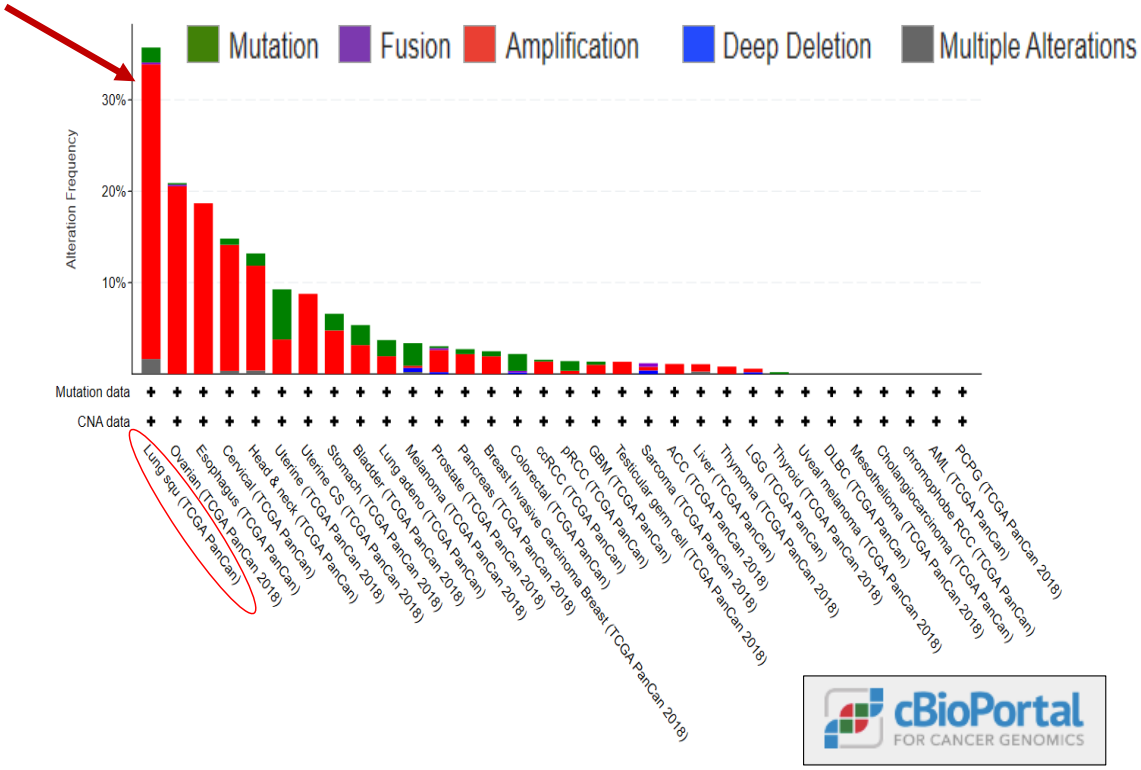

Figure 11: Patient data analysis showing altered expression and mutations in GPP130

Fig 11: Analysis of patient data obtained from cBioPortal for Cancer Genomics Database showing altered expression and/or acquired mutations of GPP130 in cancer patients. According to this chart, lung cancer patients had over 30% amplification of GPP130, suggesting this protein may have implications in the progression of lung cancer.

Chapter 1.3.1 –Shiga toxicosis

Shiga-Toxicosis is a severe gastro-intestinal disease caused by Shiga-toxin (Stx) producing E.Coli (STEC) affecting children and elderly groups of people in industrialized countries. It affects over 150 million people worldwide, and its symptoms range from diarrhea with blood to hemorrhagic colitis to Hemolytic Uremic Syndrome (HUS), kidney failure and neurological disorders. STEC is usually transmitted by the consumption of raw or undercooked meat and/or cross-contaminated vegetables [57].

It is well known that antibiotic treatment in bacteria induces a bacterial distress response, subsequently initiating the production and release of phages from the bacteria, including factors that improve survival and continuous replication even in the presence of extensive DNA damage. For this reason, the use of antibiotics for the treatment of Shiga-Toxicosis is controversial as it may pose a risk for increased production of Stx, and therefore the current treatment strategies include supportive treatments like rehydration therapy or dialysis when applicable [57]. A study by Mukhopadhyay S. et al. in 2013 revealed that Shiga-toxin binds to the luminal domain of GPP130, upon which GPP130 sorts this complex to the Golgi - Endoplasmic Reticulum, where the toxin exerts its cytotoxic effects [55]. In 2010, researchers from Carnegie Mellon University, discovered Manganese, an element found in nature, that can neutralize the lethal effects of Shiga toxin infections [54].

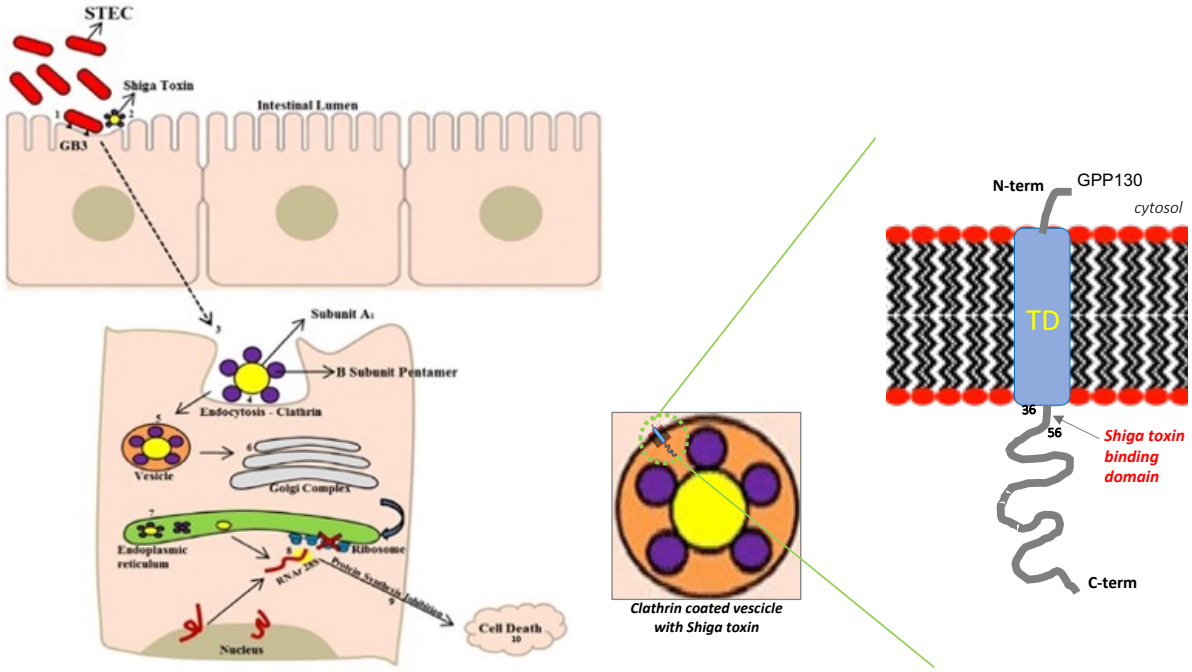

Figure 12: Mechanism of Shiga-Toxin infections

Fig 12: *(LEFT)* **S**higa-**T**oxin producing **E**scheria **C**oli (STEC) bacteria binds to Globotriaosylceramide (GB3) lipid layer of the cell$_{Step1}$ and starts to produce Shiga-toxin (Stx)$_{Step2}$. The toxin enters the cell through endocytosis$_{Step3,4,5}$ and is transported to the Golgi complex in a Clathrin coated vesicle$_{Step6}$. The vesicle breaks upon reaching the Golgi complex, disassociating the Stx structure into B subunit pentamer and subunit A1$_{Step7}$. The A1 interacts with the 28S subunit of ribosomal RNA, preventing RNA translation, eventually causing cell death. Illustration adapted from Castro et al., *Comprehensive Reviews in Food Science and Food Safety*, 2017[58]

(RIGHT) GPP130 contains both Golgi and Endosomal retrieval determinants. GPP130 is present on the surface of the endosomes when Stx is internalized into the cell. The B subunit of Stx binds to GPP130 at its luminal domain, upon which the GPP130-Stx complex is sorted to the Golgi Complex [55].

Chapter 1.3.2 – Preliminary data on GPP130 shedding by PCs

As aforementioned, our laboratory performed a quantitative proteomics screen analysis of the N-glycosylated polypeptides secreted from HuH7 (hepatic carcinoma) cells, thus identifying GPP130 as a PC7/Furin substrate.

Additionally, upon performing biochemical studies of GPP130, our laboratory, using immunofluorescence co-localization techniques, showed that GPP130 is predominantly localized in the TGN (Trans Golgi Network). Our laboratory also revealed that among all PCs, only PC7 and Furin can cleave GPP130 at different sites generating two soluble secreted forms, S1 (100kDa) and S2 (75kDa). PC7 cleaves GPP130 at **HR**S**R$_{70}$**↓LE, and Furin cleaves at H**R**S**R**$_{70}$LE**K**$_{73}$↓SL, generating S1. Additionally, Furin also cleaves GPP130 at **K**PT**R$_{277}$**↓EV generating S2. Finally, data from our laboratory also revealed that upon Manganese treatment, GPP130 undergoes conformational changes, which alters S1 and S2 cleavage by PC7 and Furin before its subsequent degradation in the lysosomes.

The data presented in this thesis expands on the aforementioned preliminary results and further investigates the implication of GPP130 in the progression of lung cancer.

Chapter 2 – Hypothesis & Objectives

In the CASC4 study, our laboratory reported that the overexpression of CASC4 decreases cell migration and invasion in triple-negative breast cancer (TNBC) cells. Additionally, the study showed that the membrane-bound N-terminal fragment of CASC4, generated upon its shedding by PC7/Furin, caused drastic re-organization of the actin cytoskeleton and resulted in enhanced migration and invasion of TNBC cells [43].

Hence, we propose GPP130, just like CASC4, may have a role in the tumorigenesis of lung cancer and that its shed forms may be implicated in lung cancer proliferation.

The objectives of this study are as follows:

- Investigate the expression levels of GPP130 in A549 Lung Cancer cells.
- Investigate the impact on proliferation by overexpression and knockdown of GPP130 in A549 lung cancer cells.
- Identify the effect of GPP130 shedding by PC7/Furin on cellular proliferation.
- Identify the region of GPP130 that confers a proliferative advantage to these cells.
- Identify other potential Post-Translational Modifications that could further confer a proliferative advantage.
- Investigate the presence of negative regulators of GPP130-induced cellular proliferation.
- Investigate possible therapeutic strategies against A549 Lung Carcinoma cells expressing GPP130.

Chapter 3 – Materials and Methodology

Plasmids

Human **GPP130 WT**, **GPP130 aa(1-67)**, **GPP130 aa(278-696)**, **soluble GPP130** (Signal peptide - aa (71-696)- lacking the transmembrane domain; ΔTM), **GPP130 SP-aa(71-277)**, full-length human PC7, full-length human Furin cDNAs were cloned V5 tag at the C-terminus, into pIRES-EGFP vector (Clontech). Site-directed mutagenesis was used to generate G2A, C6A, G2AC6A, R70A in full-length GPP130. GPP130 (EH**R**S**R**$_{70}$LE) was mutated to **RRRRR**$_{70}$E**L** (5REL) to generate a Furin/PC7 optimized cleavage site. A PC uncleavable mutant, GPP130 (R70AR277A), was generated via site-directed mutagenesis.

Cell Culture and cDNA transient transfections

A549 cells were grown in Kaighn's Modification of Ham's F-12 Medium (F12K, Invitrogen) supplemented with 10% Fetal Bovine Serum (Wisent) and 1% Penicillin-Streptomycin (Sigma). HEK293 cells were grown in Dulbecco's modified Eagle's medium (DMEM, Invitrogen) with 10% FBS, Invitrogen. All cells were maintained at 37°C under 5% CO_2. HEK293 cells were transiently co-transfected with equimolar quantities (0.5µg) of each plasmid using Jetprime Polyplus, whereas A549 cells were transfected with equimolar quantities (1.0µg) of each plasmid using FuGene HD, using the manufacturer's instructions.

Cell treatments

At 24 hours post-transfection, cells were washed in serum-free medium followed by additional 24 hours alone or incubation with 20mM NH4Cl or 10uM D6R, 75uM dec-

RVKR-cmk, 0.1 uM Boston Pharmaceutical compund 318 and 1.0 uM Boston Pharmaceutical Compound 318 (BOS318)

Western Blot Analysis and Antibodies

Proteins were extracted in RIPA buffer with cocktails of protease inhibitors (Roche). Bradford assay was used to evaluate the protein concentrations. Proteins were resolved on SDS-PAGE and blotted onto nitrocellulose membranes. The following primary and secondary antibodies were used to incubate the membrane: Mouse anti-V5 (1:5000, Invitrogen), rabbit anti-β-actin (1:5,000, Sigma-Aldrich), or horseradish peroxidase (HRP)-conjugated mAb V5 (1:10,000, Sigma-Aldrich). Quantifications were done using the ChemiDoc imaging system (Biorad).

Cell Proliferation Analysis

For cell proliferation assays, cells were seeded into a 24-well plate (Greiner) at low cellular density (15,000 cells/well) and placed into the Incucyte imager for up to 96 hours. Images were taken by the machine at intervals of 12 hours to generate cellular density (% of confluence), and results were graphed over time.

Each experiment was performed at least n=2 times in duplicates or triplicates, and subsequent statistical analysis was done using the Students t-test wherein

***** means $p \leq 0.05$; ****** means $p \leq 0.01$; ******* means $p \leq 0.001$ and

ns means $p > 0.05$.

All data are presented as the mean and the error bars as SD (Standard Deviation).

Chapter 4 – RESULTS

4.1. Shedding of GPP130 at S1 and S2 occurs inside the cell

Among the members of the PC family, our laboratory showed that GPP130 is uniquely cleaved by PC7 at **HR**S**R**$_{70}$↓LE (S1) and by Furin at **HR**S**R**$_{70}$LE**K**$_{73}$↓ (S1) and **K**PT**R**$_{277}$↓EV (S2).

Since both PC7 and Furin can traffic to the plasma membrane to cleave substrate proteins, we investigated if GPP130 is shed at the plasma membrane by treating HEK293 cells overexpressing GPP130 and PC7/Furin with 75uM cell-permeable pan-PC general inhibitor, Decanoyl-RVKR-cmk (RVKR) and 10uM non-cell-permeable inhibitor, hexapeptide (D-Arg$_6$) (D6R).

The data obtained upon treatment with 75uM RVKR shows the abolishment of S1 cleavage by both PC7 and Furin, suggesting that S1 cleavage occurs inside the cell. However, no decrease in S2 shedding by Furin was observed, indicating that S2-shedding is not affected by this pan-PC inhibitor, which may occur in endosomes, not permeable to RVKR treatment (Figure 13A). Furthermore, the data suggest that cleavage at S2 by Furin does not necessarily require a prior cleavage at S1, revealing that these are independent cleavages. In contrast, the data obtained upon D6R 10uM treatment shows no change in either S1 or S2 shedding, suggesting that both cleavages do not occur at the cell surface (Figure 13B).

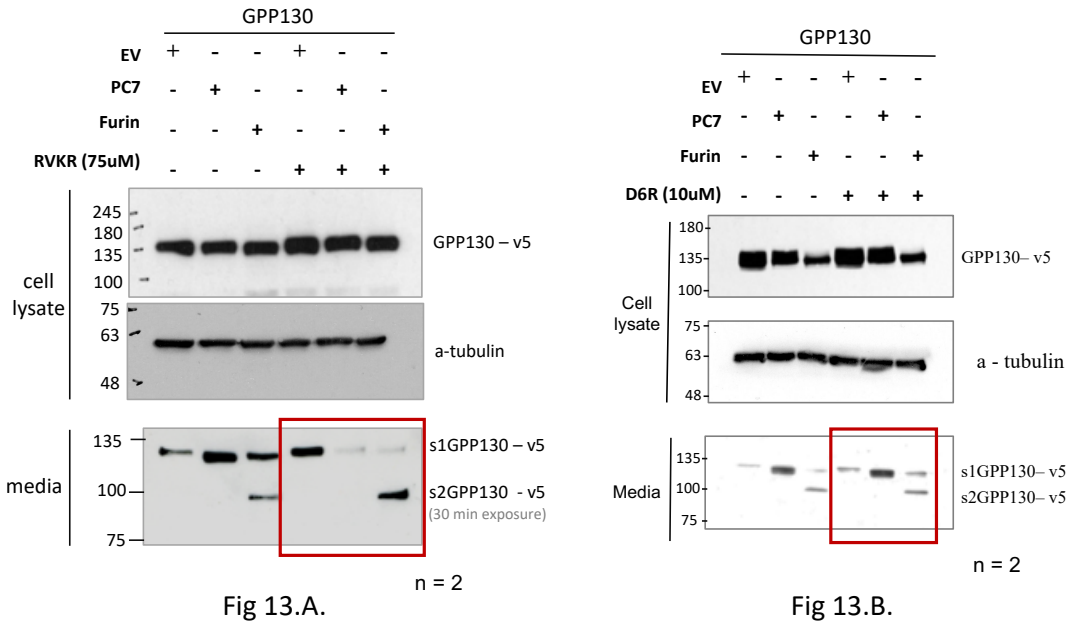

Figure 13: Shedding of GPP130 s1 and s2 occurs inside the cell

Fig 13: A. Western blot analysis of cells lysates and media from HEK293 cells overexpressing GPP130-V5 WT, with human PC7, human Furin or with pIRES-Empty Vector treated with RVKR (75uM). Highlighted in red are the differences in s1 and s2 shed fragments upon RVKR treatment.

B. Western blot analysis of cells lysates and media from HEK293 cells overexpressing GPP130-V5 WT, with human PC7, human Furin or with pIRES-Empty Vector treated with D6R (10uM). Highlighted in red are the differences in s1 and s2 shed fragments upon D6R treatment.

4.2. GPP130 shedding by PC7 and Furin occurs in acidic compartments of the cell

To further understand which cellular compartment this cleavage occurs, we treated HEK293 cells overexpressing GPP130 and PC7/Furin with 20mM NH_4Cl, an alkylating agent that blocks the acidification of intracellular compartments, to check if the cleavage occurs in acidic pH compartments. Our results show that NH_4Cl treatment prevented the PC7 and Furin cleavages of both S1 and S2 (Figure 14), suggesting that S1 and S2 cleavages occur in acidic compartments like the TGN and/or endosomes. It is important

to note the presence of a very faint S2 band with NH4Cl treatment. This may be due to a high exposition time during the development of the X-Ray film. The higher molecular weight protein band seen in the media in absence and especially in the presence of NH_4Cl may be due to exosome secretion of the full-length GPP130 protein.

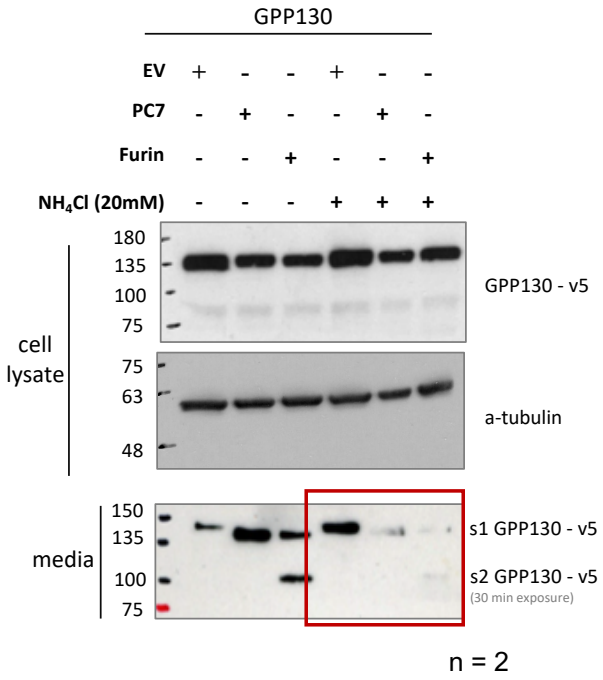

Figure 14: GPP130 shedding by PC7 and Furin occurs in acidic compartments of the cell

Fig. 14: Western blot analysis of cells lysates and media from HEK293 cells overexpressing GPP130-V5 WT, with human PC7, human Furin or with pIRES-Empty Vector treated with Nh_4Cl (20mM).

4.3. A549 cells express GPP130, PC7 and Furin

GPP130 is amplified in ~35% of lung cancer patients, as depicted in Figure 11. Keeping this in mind, we decided to use A549 lung carcinoma cell line, derived from the lung tissue of a Non-Small Cell Lung Cancer (NSCLC) patient, for all subsequent cell-culture experiments. They are the most commonly used human NSCLC cell line in basic research and consist of hypotriploid alveolar basal epithelial cells, squamous in nature. As A549

cells are commonly employed as a model for investigating the progression of lung cancer, we opted to utilize this cell line for our forthcoming cellular investigations as well.

Before performing any experiment in these cells, we sought to measure the mRNA expression levels of GPP130, PCSK7 and Furin. We extracted RNA from A549 cells after letting them grow for 24 hours. Quality-check of the extracted RNA was done by agarose gel electrophoresis, and the corresponding cDNA was generated by RT-PCR.

To analyze the mRNA expression of GPP130, PSCK7 and Furin, qPCR was performed.

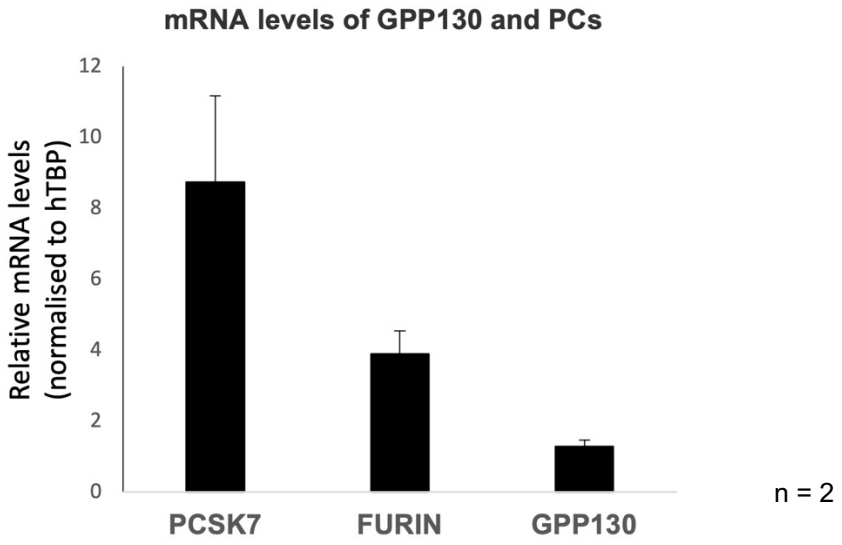

Figure 15: mRNA expression levels of GPP130, PSCK7 and Furin

Fig. 15: The bar graph shows the levels of mRNA expression of hGPP130, hPCSK7 and hFurin relative to hTBP (human TATA box Binding Protein) in A549 lung carcinoma cells.

The data obtained shows mRNA expression levels of the three genes normalized to human TATA box Binding Protein (hTBP). We show A549 cells express high levels of PCSK7 (8.75 times hTBP), moderate levels of Furin (3.89 times hTBP) and GPP130 (1.28 times hTBP) (Figure 15).

Since A549 cells express PCSK7, Furin and GPP130, we carried subsequent cell culture experiments with these cells.

4.4. Density gradient curve of A549 Cells

Before performing cell proliferation experiments, we wanted to optimize the cell density of human A549 cells (derived from a type II pneumocyte lung tumor) that can grow to 100% confluency in 96 hours. For this, we seeded A549 cells at different cell concentrations (15K, 30K, 45K,60K, 65K, 90K, 105K, 120K cells/well) in a 48-well plate and tracked their confluency over time. Additionally, we decided to run every experiment for 96 hours because transient cDNA over-expressions / siRNA transfections / various drug treatments, require at least 48 hours to be fully activated and an additional 48 hour period for the cells to grow seemed optimum.

The results of this preliminary experiment show that 15,000 cells/well in a 48-well plate grow to 100% confluency in 96 hours (red curve; Figure 16).

We used this density graph as a reference for all future experiments henceforth.

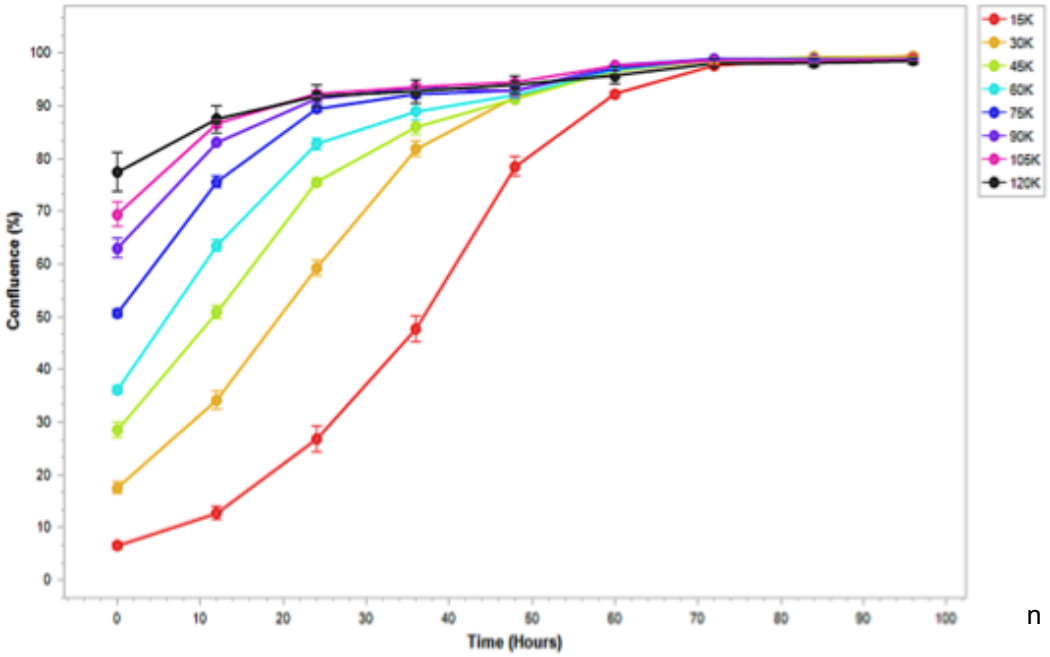

n = 2

Figure 16: Density Gradient curve of A549 lung carcinoma cells

Fig. 16: Growth curves of A549 cells seeded at different cell concentrations and allowed to proliferate for 96 hours. This graph illustrates that a seeding concentration of 15,000 cells/well is optimum for cell culture experiments on A549 cells.

4.5. Overexpression of GPP130 increases proliferation

Upon analyzing patient data from a genomics database (cBioPortal for Cancer Genomics), we noted that the *Golim4* gene is amplified in up to ~35% of lung cancer patients. Taking this into context, we henceforth decided to use A549 lung carcinoma cells to perform all the proliferation assays.

Primarily we wanted to check if overexpression of GPP130 in A549 cells can enhance proliferation compared to the WT A549 cells. Thus, we overexpressed the cDNA encoding WT GPP130 in A549 cells and let the experiment run for 96 hours.

Our results show that at 96h, overexpression of GPP130 results in a ~20% increase in A549 cells (purple curve) compared to overexpression of the pIRES EV (Figure 17).

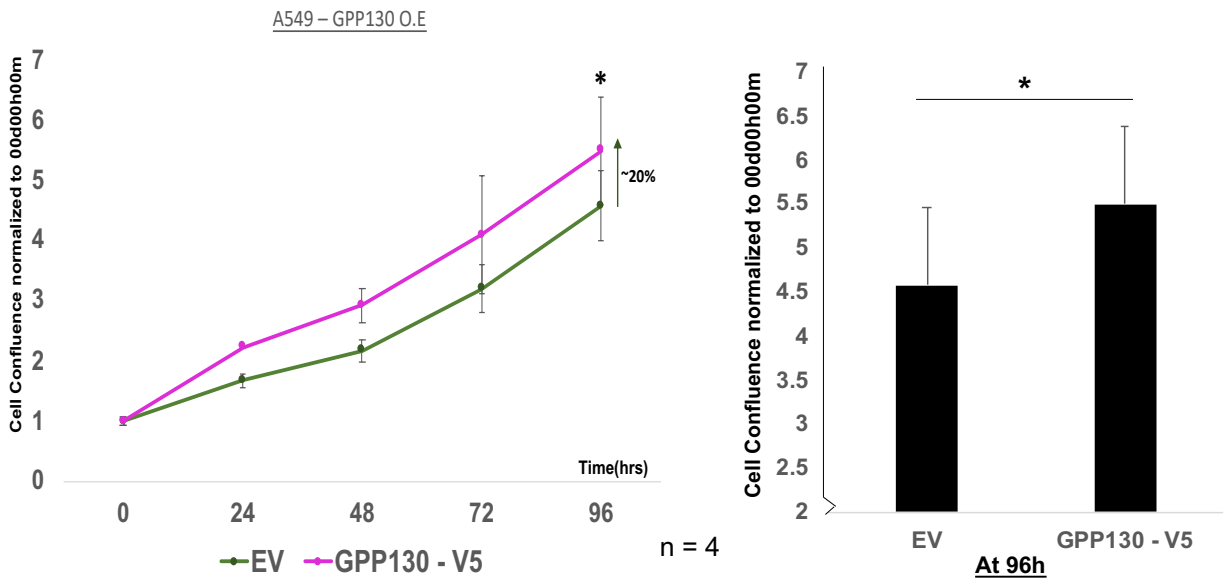

Figure 17: Overexpression of GPP130 increases proliferation

Fig. 17: *(LEFT)* Growth curve of A549 cells overexpressing GPP130-V5 and pIRES-V5 empty vector normalized to scan 00d00h00m. These results are representative of four independent experiments. (ns means p>0.05), (* means p <0.05), (** means p < 0.01) and (*** means p < 0.001) (Student's t test).

(RIGHT) Corresponding bar graph of cell growth at 96 hours.

4.6. GPP130 knockdown reduces proliferation

After noticing that overexpression of GPP130 increases proliferation in A549 cells, we decided to perform a knockdown of GPP130 to validate the effects of siGPP130 on cell proliferation. A549 cells were treated with 5uM siScramble and 5uM siRNA of GPP130 and allowed to grow for 90 hours. In line with the pro-proliferative activity of WT GPP130 (Fig. 17), the results of this experiment showed a ~35% decrease in the proliferation of A549 cells lacking endogenous expression of GPP130 (orange curve; Figure 18).

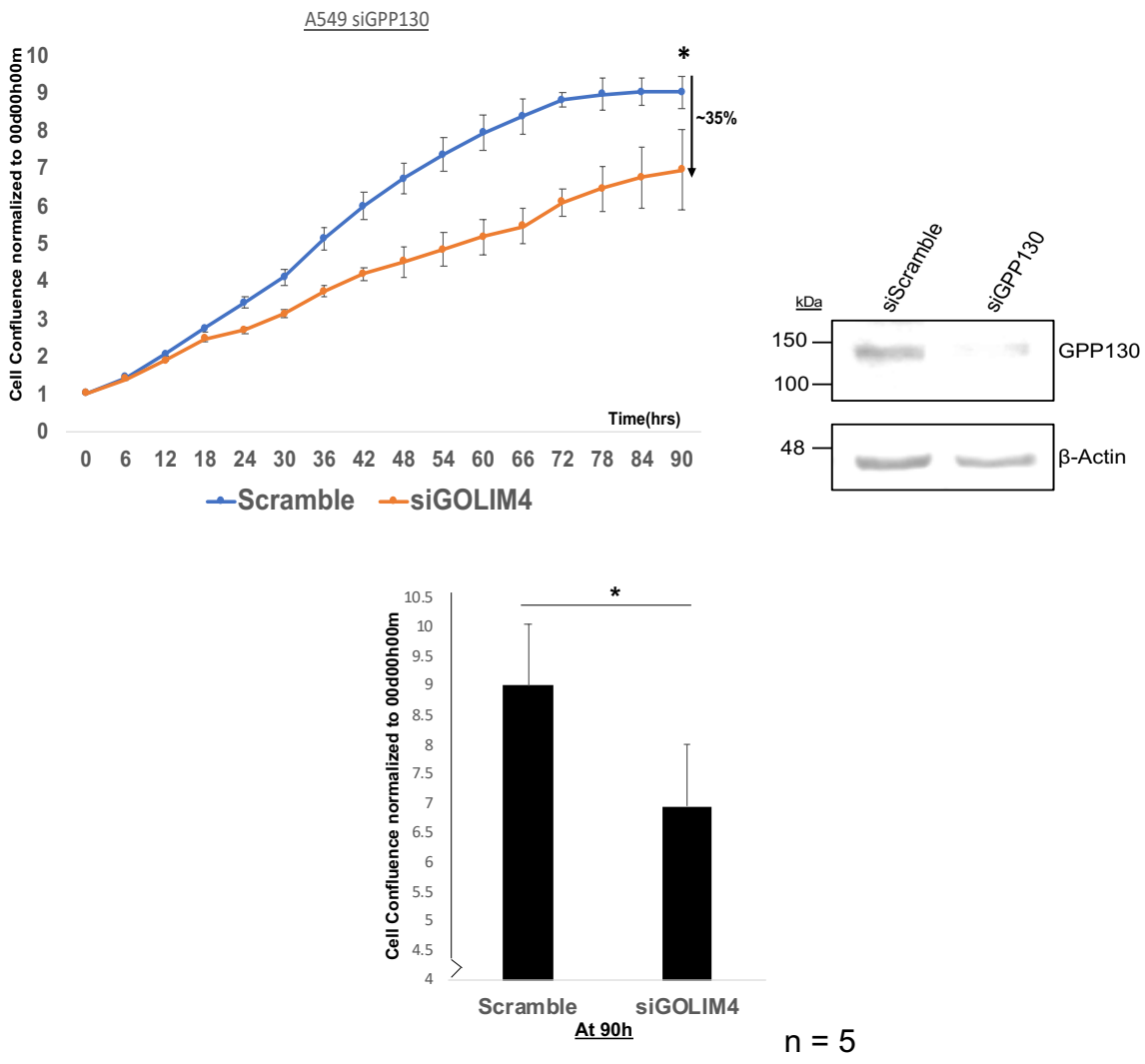

Figure 18: GPP130 knockdown reduces proliferation

Fig. 18: The figure shows (i) **the** Growth curve of A549 lung cancer cells following siRNA for GPP130 or Scramble control over a period of 96 hours, showing a 35% decrease in cell growth upon siGPP130 transfection. (ii) Western blot analysis of cell lysates from A549 cells following siRNA for GOLIM4 or Scramble control over a three-day period. (iii) Corresponding bar graph of cell growth at 96 hours. These results are representative of five independent experiments. (ns means p>0.05), (* means p <0.05), (** means p < 0.01) and (*** means p < 0.001) (Student's t test).

4.7. GPP130 shedding by endogenous PCs shows an upward trend in proliferation

To observe if shedding of GPP130 by PC7 at **HRSR**$_{70}$↓LE (S1) and by Furin at **HRSR**$_{70}$LE**K**$_{73}$↓ (S1) has an impact on cell proliferation, we generated an S1 optimally cleaved mutant of Full Length GPP130 by mutating the sequence from EHRSR$_{70}$LE to **RRRRR**$_{70}$EL so that GPP130-5REL can be optimally cleaved by endogenous PC7 and Furin. We also generated GPP130 R70A mutant to prevent S1 shedding by PC7 at R$_{70}$ and Furin at R$_{73}$ by mutating R (arginine) to A (alanine), as this woud place Ala at the P1 and P4 positions of PC7 and Furin, respectively.

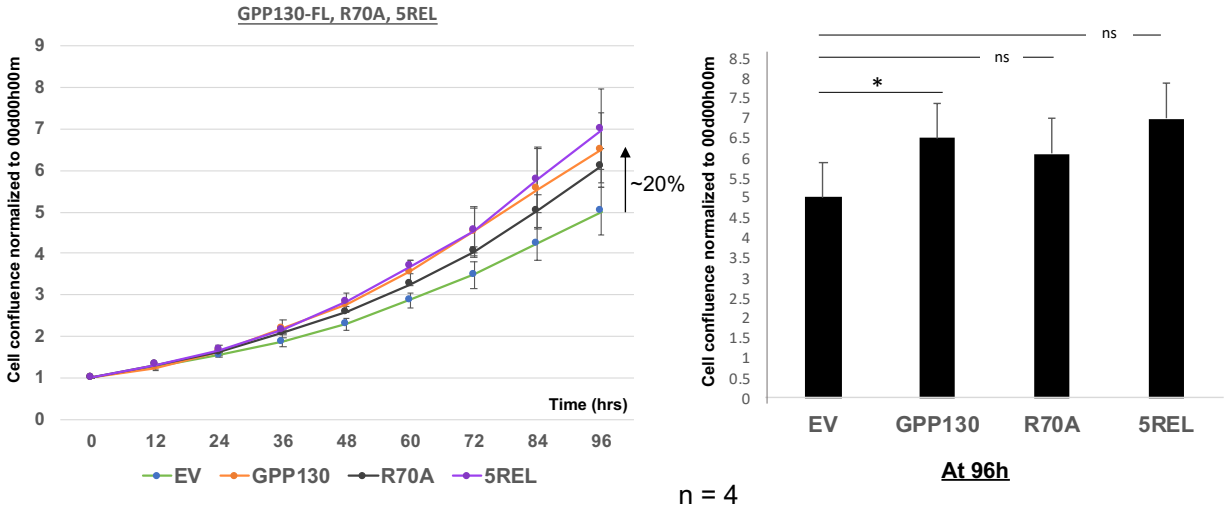

Figure 19: Shedding of GPP130 by PCs shows an upward trend in proliferation

Fig 19: This diagram illustrates (LEFT) the growth curve of A549 cells upon overexpression of pIRES-V5 EV, GPP130-FL, GPP130 5REL and GPP130 R70A and allowed to proliferate for 96 hours. GPP130 5REL showed enhanced growth in comparison to pIRES-V5 EV, as expected. GPP130 R70A also showed enhanced growth, suggesting that this is due to the generation of GPP130 aa(1-276) after cleavage of GPP130 at S2 by Furin. *(RIGHT)* Corresponding bar graph of cell growth at 96 hours. This experiment has been done n=1 times. . (ns means p>0.05), (* means p <0.05), (** means p < 0.01) and (*** means p < 0.001) (Student's t test).

We then overexpressed 0.5ug cDNA of GPP130-FL, GPP130R70A, GPP130REL and pIRES EV and let the experiment run for 90 hours.

Although not statistically significant, the data obtained showed that the overexpression of the GPP130-5REL mutant resulted in an upward trend (p=0.052) of A549 cell proliferation (purple curve), higher than EV and GPP130-FL, indicating that GPP130 shedding by PCs results in increased cellular growth.

Additionally, we also noticed the increase in proliferation upon the overexpression of GPP130-R70A (S1 uncleavable mutant) (black curve). Although in this mutant GPP130 S1 cleavage is prevented, S2 can still be cleaved at **K**PT**R**$_{277}$↓EV by Furin, leading us to hypothesize that this increase is due to the generation of GPP130 (1-276) fragment after possible cleavage of GPP130 at **K**PT**R**$_{277}$↓EV by Furin.

A future experiment proposed is to co-transfect the cDNAs of GPP130-FL with those of PC7 or Furin, as the endogenous levels of PC7 or Furin may not be high enough to substantially cleave overexpressed GPP130. If the data obtained from this experiment shows an upregulated proliferation of A549 cells, we can further confirm that GPP130-induced proliferation requires PC cleavage activity on GPP130.

4.8. Generation of GPP130 constructs

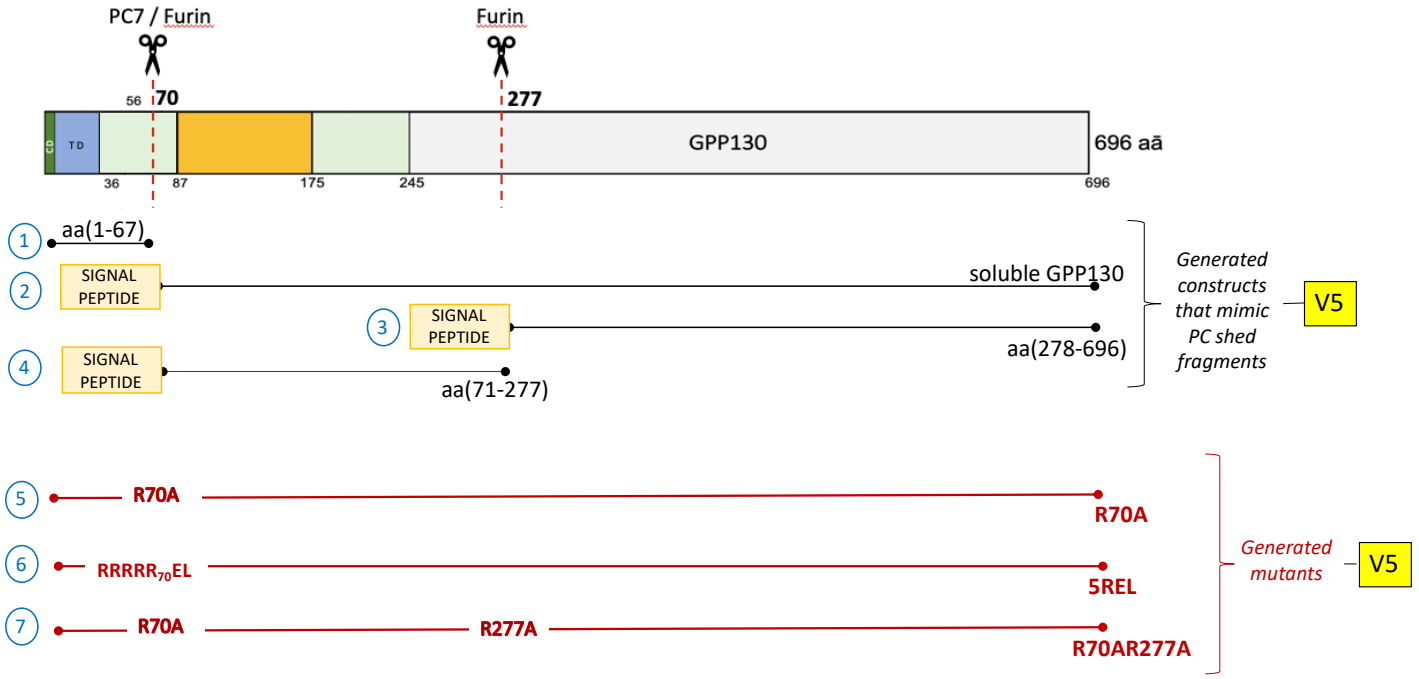

Figure 20: Schematic representation of various GPP130 constructs

Fig 20: This diagram illustrates the generated GPP130 constructs and GPP130 mutants. All these constructions were tagged with V5 at the C-terminus and inserted into the pIRES plasmid.

To confirm if GPP130 shedding by PCs impacts cellular proliferation, we generated GPP130 fragments that mimic its shedding by PCs. We also constructed fragments to understand better the region of the GPP130 protein that induces proliferation in A549 cells. These constructs were generated tagged with a V5 at their C-terminus end, described as follows:

1) **GPP130aa(1-67)-V5** – N-terminal membrane-bound fragment of GPP130 generated upon cleavage by PC7 at **HR**S**R**$_{70}$↓LE.

2) **spPCSK9 - Sol.GPP130-ΔTM-V5 –** Secreted luminal domain protein fragment of GPP130 containing PCSK9 signal peptide to mimic the secreted fragment generated upon cleavage by PC7 at **HR**S**R**$_{70}$↓LE.

3) **spPCSK9-GPP130 aa(278-696)-V5 –** Secreted luminal domain protein fragment of GPP130 containing PCSK9 signal peptide to mimic the secreted fragment generated upon cleavage by Furin at **K**PT**R**$_{277}$↓EV.

4) **spPCSK9-GPP130 aa(71-277)-V5 –** soluble sub-fragment of GPP130-ΔTM. *(in progress)*

5) **GPP130-R70A-V5 –** GPP130 mutant resistant for PC shedding at S1. It prevents both PC7 cleavage at **HR**S**R**$_{70}$↓LE and Furin cleavage at **HR**S**R**$_{70}$LE**K**$_{73}$↓ since Arginine$_{70}$ (R) is mutated to Alanine$_{70}$ (A).

6) **GPP130-5REL-V5** – S1 optimally cleaved mutant of full-length GPP130 generated by mutating the sequence from E**HR**S**R**$_{70}$LE to **RRRRR**$_{70}$EL.

7) **GPP130-R70A277A-V5** – GPP130 mutant resistant for PC shedding at S1 and S2. It prevents PC7 cleavage at **HR**S**R**$_{70}$↓LE and Furin cleavage at both **HR**S**R**$_{70}$LE**K**$_{73}$↓ and **K**PT**R**$_{277}$↓EV since R$_{70}$ and R$_{277}$ are mutated to A$_{70}$ and A$_{277}$. *(in progress)*

These constructs and mutants are tagged with V5 at their C-terminus and were inserted into the **pIRES** expression plasmid.

4.9. Soluble GPP130-ΔTM increases proliferation

To observe the region of the GPP130 luminal domain that is able to induce cellular proliferation, we co-expressed cDNAs encoding GPP130 constructs **GPP130(FL), GPP130aa(1-67), Sol.GPP130-ΔTM**, **GPP130aa(278-696)** and **pIRES EV** in a 24-well plate in A549 cells and the cell growth was tracked for 96 hours. Our results show that only the overexpression of the Sol.GPP130ΔTM (blue curve), which mimics GPP130-PC7 shed fragment, significantly promoted A549 cell proliferation in comparison to GPP130(FL), suggesting that the GPP130 fragment generated upon shedding by PC7 can be deleterious (Figure 21).

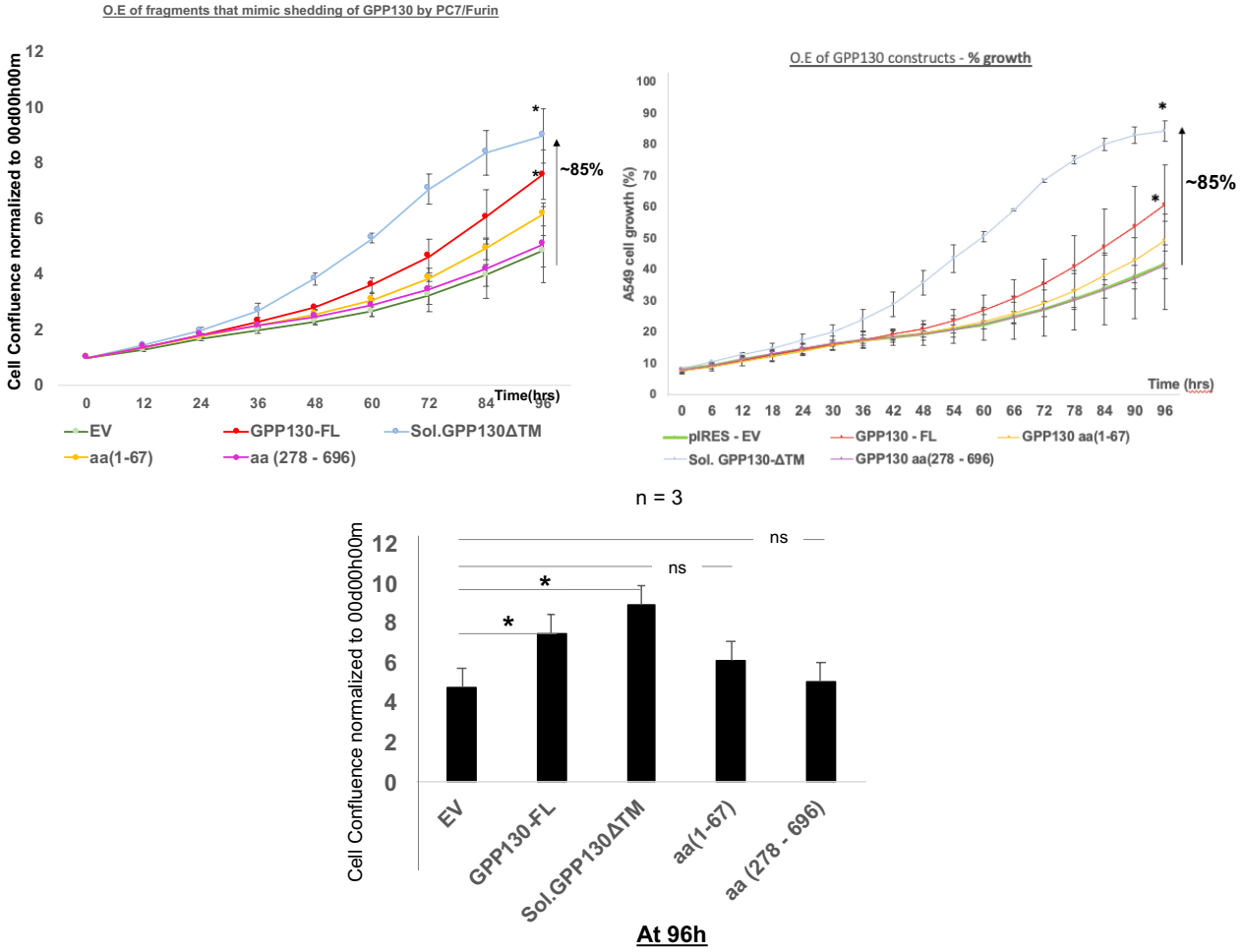

Figure 21: Soluble GPP130-ΔTM increases proliferation

Fig. 21: *(TOP)* The figure shows the growth curve of A549 lung cancer cells overexpressing pIRES-V5 EV, GPP130-ΔTM, GPP130 aa(1-67), GPP130 aa(278-696) and allowed to proliferate for 96 hours. GPP130-ΔTM showed enhanced growth compared to pIRES-V5 EV, growing at double the rate. The graphs presented show both the (left) ratio of growth to 00d00h00m and (right) percentage of growth.

(BOTTOM) Corresponding bar graph of cell growth at 96 hours. These results are representative of three independent experiments. (ns means p>0.05), (* means p < 0.05), (** means p < 0.01) and (*** means p < 0.001) (Student's t test).

4.10. Sol.GPP130-ΔTM media swap increases proliferation

After observing that Sol.GPP130-ΔTM promotes cellular proliferation, we decided to perform a media swap experiment. A549 cells were co-expressed with cDNAs of Sol.GPP130-ΔTM and pIRES EV. After 24 hours, media from the respective wells were collected. This media was then added to naïve A459 cells along with F12K complete media (1:1) and allowed to grow for 96 hours. The results from this experiment showed that a media swap of Sol.GPP130-ΔTM can induce significant, albeit small, cellular proliferation (orange curve) (Figure 22).

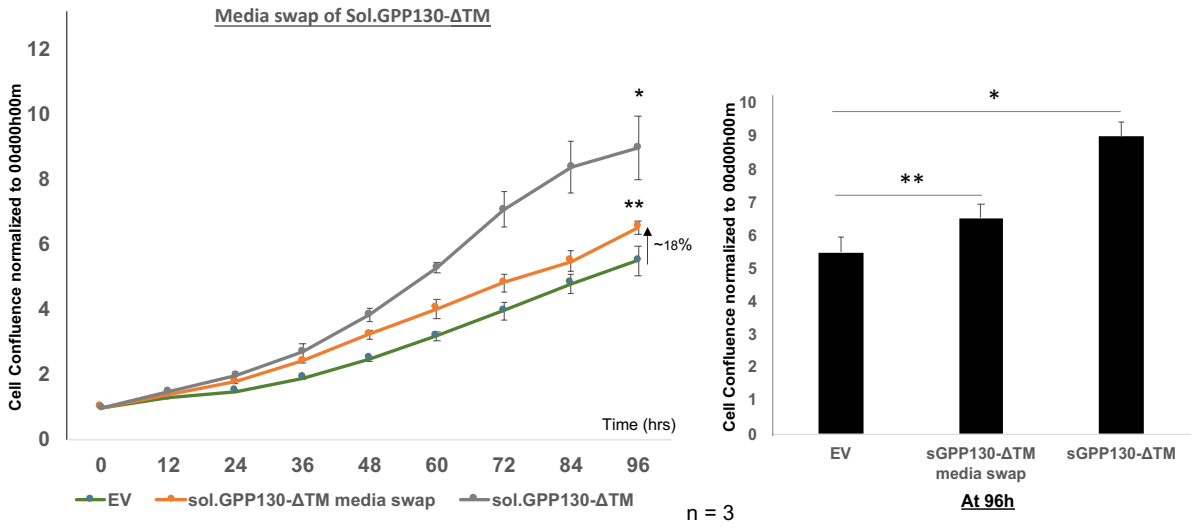

Figure 22: Soluble GPP130-ΔTM media swap increases A549 cell proliferation

Fig. 22: *(LEFT)* The figure shows the growth curve of A549 lung cancer cells upon treatment with media containing soluble GPP130-ΔTM fragment.

(RIGHT) Corresponding bar graph of cell growth at 96 hours. These results are representative of three independent experiments. (ns means p>0.05), (* means p <0.05), (** means p < 0.01) and (*** means p < 0.001) (Student's t test).

4.11. Sortilin is a negative regulator of Sol.GPP130- ΔTM induced proliferation

Venkat S. et al. showed that Manganese-induced/ trafficking and turnover of GPP130 is mediated by Sortilin [59]. We hypothesized that Sortilin might also be able to negatively regulate proliferation induced by over-expressed Sol.GPP130-ΔTM. We then performed transient transfection of cDNAs encoding Sortilin and Sol.GPP130-ΔTM in equimolar quantities and let the cells grow for 96 hours. As hypothesized, overexpressing sortilin along with Sol.GPP130-ΔTM reduced cellular proliferation (Figure 23), suggesting that Sortilin potentially binds to Sol.GPP130-ΔTM and trafficks the complex to lysosomes for degradation.

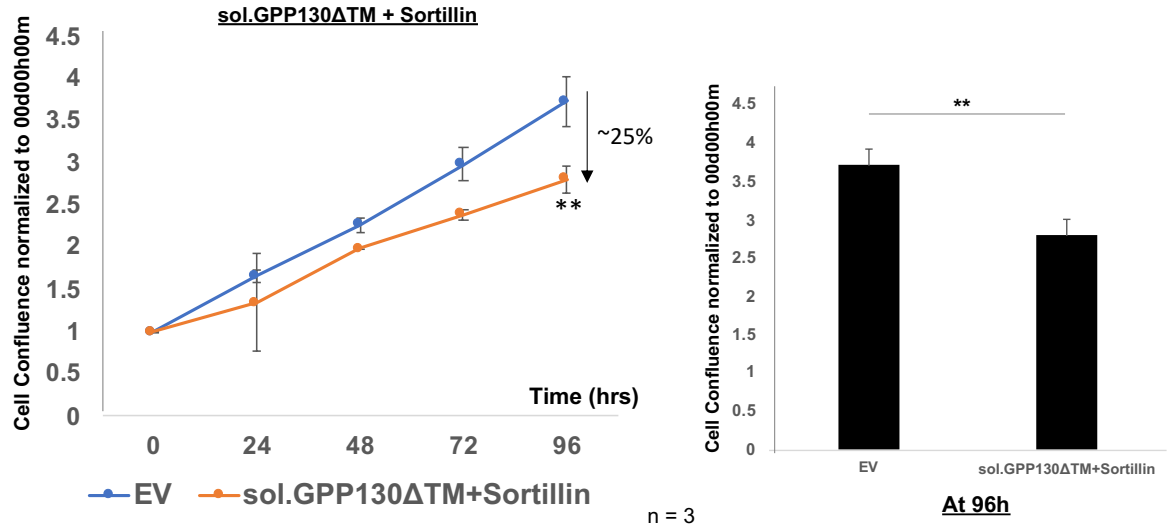

Figure 23: Sortilin is a negative regulator of Soluble GPP130- ΔTM induced proliferation

Fig. 23: *(LEFT)* The figure shows the growth curve of A549 lung cancer cells co-expressing equimolar quantity of soluble GPP130-ΔTM fragment and Sortilin, and pIRES-V5 EV.

(RIGHT) Corresponding bar graph of cell growth at 96 hours. These results are representative of three independent experiments. (ns means p>0.05), (* means p <0.05), (** means p < 0.01) and (*** means p < 0.001) (Student's t test).

4.12. Lipid modifications of GPP130 N-term domain

Upon examining the sequence of human GPP130, we observed potential sites for lipid modifications at its N-terminal domain. We noticed that Gly_2 was a possible site for the addition of myristic acid by N-Myristoyltransferase (NMT). Additionally, we also noticed Cys6, a potential site for palmitoylation by Protein Palmitoylatransferases (PATs).

```
        10         20         30         40         50         60
MGNGMCSRKQ KRIFQTLLLL TVVFGFLYGA MLYYELQTQL RKAEAVALKY QQHQESLSAQ
        70         80         90        100        110        120
LQVVYEHRSR LEKSLQKERL EHKKAKEDFL VYKLEAQETL NKGRQDSNSR YSALNVQHQM
       130        140        150        160        170        180
LKSQHEELKK QHSDLEEEHR KQGEDFSRTF NDHKQKYLQL QQEKEQELSK LKETVYNLRE
       190        200        210        220        230        240
ENRQLRKAHQ DIHTQLQDVK QQHKNLLSEH EQLVVTLEDH KSALAAAQTQ VAEYKQLKDT
       250        260        270        280        290        300
LNRIPSLRKP DPAEQQNVTQ VAHSPQGYNT AREKPTREVQ EVSRNNDVWQ NHEAVPGRAE
       310        320        330        340        350        360
DTKLYAPTHK EAEFQAPPEP IQQEVERREP EEHQVEEEHR KALEEEEMEQ VGQAEHLEEE
       370        380        390        400        410        420
HDPSPEEQDR EWKEQHEQRE AANLLEGHAR AEVYPSAKPM IKFQSPYEEQ LEQQRLAVQQ
       430        440        450        460        470        480
VEEAQQLREH QEALHQQRLQ GHLLRQQEQQ QQQVAREMAL QRQAELEEGR PQHQEQLRQQ
       490        500        510        520        530        540
AHYDAMDNDI VQGAEDQGIQ GEEGAYERDN QHQDEAEGDP GNRHEPREQG PREADPESEA
       550        560        570        580        590        600
DRAAVEDINP ADDPNNQGED EFEEAEQVRE ENLPDENEEQ KQSNQKQENT EVEEHLVMAG
       610        620        630        640        650        660
NPDQQEDNVD EQYQEEAEEE VQEDLTEEKK RELEHNAEET YGENDENTDD KNNDGEEQEV
       670        680        690
RDDNRPKGRE EHYEEEEEEE EDGAAVAEKS HRRAEM
```

Figure 24: Human GPP130 sequence

Fig 24: Protein Sequence of human GPP130 obtained from UniProt

4.12.1. Myristoylation of GPP130 N-terminal domain

Upon examining the sequence of human GPP130, we noticed a Glycine at position 2 after a Methionine at position 1. This made us check if the N-terminal domain of GPP130 is potentially myristoylated using EXPASY - Myristylation tool.

The results showed that the N-terminal membrane-bound fragment of GPP130aa(1-67) is predicted to be myristoylated at Gly_2 (Figure 25).

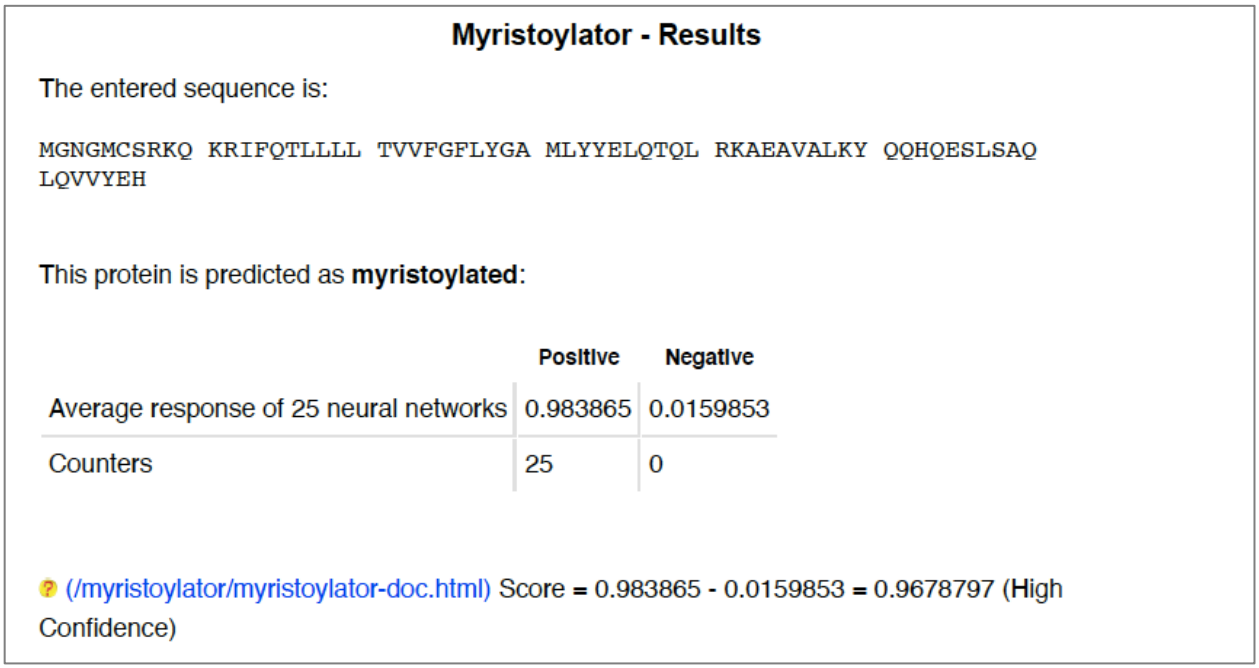

Myristoylator - Results

The entered sequence is:

MGNGMCSRKQ KRIFQTLLLL TVVFGFLYGA MLYYELQTQL RKAEAVALKY QQHQESLSAQ
LQVVYEH

This protein is predicted as **myristoylated**:

	Positive	Negative
Average response of 25 neural networks	0.983865	0.0159853
Counters	25	0

(/myristoylator/myristoylator-doc.html) Score = 0.983865 - 0.0159853 = 0.9678797 (High Confidence)

Figure 25: N-term domain of GPP130 is predicted to be Myristoylated

Fig 25: EXPASY prediction of myristoylation of the N-Terminal domain of GPP130. The data shows the sequence of GPP130 aa(1-67) is predicted to be myristoylated.

By replacing Gly_2 with Ala_2 using site-directed mutagenesis, we were able to generate a mutant of GPP130 aa(1-67), that is, GPP130 aa(1-67)G2A, that cannot be myristoylated. To analyze if this lipid modification affects the ability of cells to proliferate, we seeded A549 cells in a 24-well plate and overexpressed 0.5ug of GPP130 aa(1-67)G2A construct.

Our results show that despite being able to proliferate slightly more than EV, there is no significant difference in proliferation compared to GPP130 aa(1-67), suggesting myristoylation of GPP130 membrane-bound N-terminal fragment has no considerable impact on proliferation (Figure 26). Further studies need to be done on the impact of blocking myristoylation of the full-length GPP130 protein (GPP130G2A) on A549 cell proliferation.

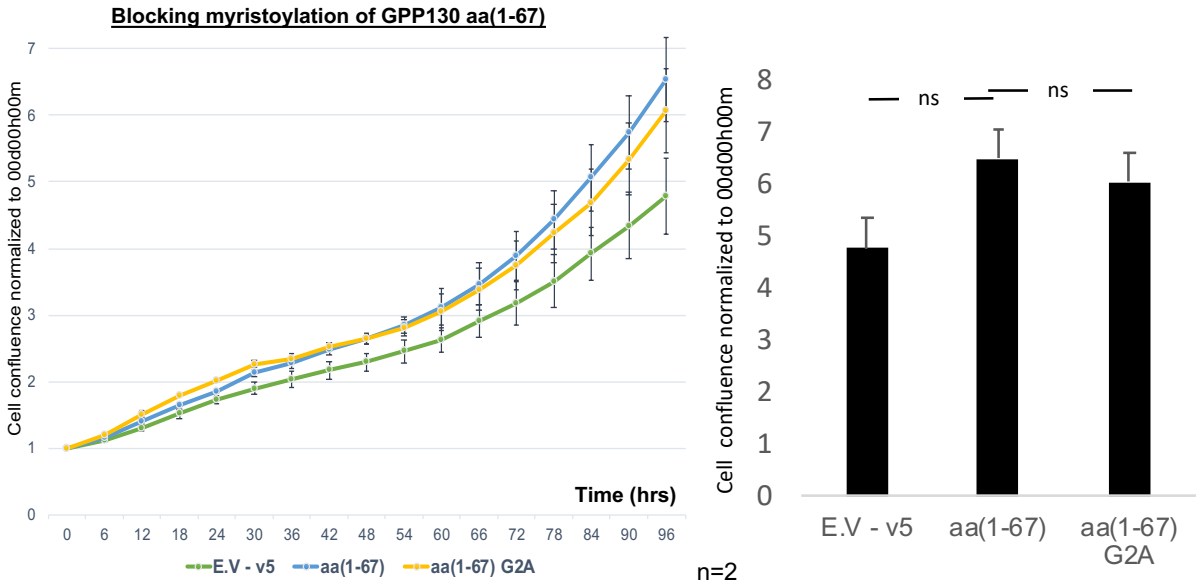

Figure 26: Blocking Myristoylation of GPP130 NTD

Fig. 26: *(LEFT)* The figure shows the growth curve of A549 lung cancer cells expressing pIRES-V5 EV, GPP130 aa(1-67)-V5 and GPP130 aa(1-67)G2A-V5 *(RIGHT)* Corresponding bar graph of cell growth at 96 hours. These results are representative of two independent experiments. (ns means $p > 0.05$), (* means $p < 0.05$), (** means $p < 0.01$) and (*** means $p < 0.001$) (Student's t test).

4.12.2. Palmitoylation of GPP130 N-term domain

In addition to observing Gly_2, we also noticed a Cys_6, a potential site of S-palmitoylation, wherein a possible covalent attachment of palmitic acid could take place.

By replacing Cys_6 with Ala_2 using site-directed mutagenesis, we were able to generate a mutant of GPP130 aa(1-67), namely, GPP130 aa(1-67)C6A that cannot be palmitoylated, that is, GPP130 aa(1-67)C6A.

To analyze if this lipid modification affects the ability of cells to proliferate, we seeded A549 cells in a 24-well plate and overexpressed 0.5ug of GPP130 aa(1-67)C6A construct. We let the experiment run for 96 hours.

The data shows that upon blocking palmitoylation of the N-term membrane-bound domain, there is a significant increase in proliferation (Figure 27). Since it is known that Palmitoylation is a dynamic process influencing protein distribution, localization, and function by modifying the protein's membrane affinity [32], we suggest that the sub-cellular localization of the non-palmitoylated fragment is potentially disturbed, causing the observed increase in A549 cell proliferation. We also suggest the possible potential downstream signalling perpetrated by GPP130(aa1-67) is regulated by palmitoylation [60] [61]. Further studies need to be done on the impact of blocking palmitoylation of the full-length GPP130 protein (GPP130C6A) on A549 cell proliferation.

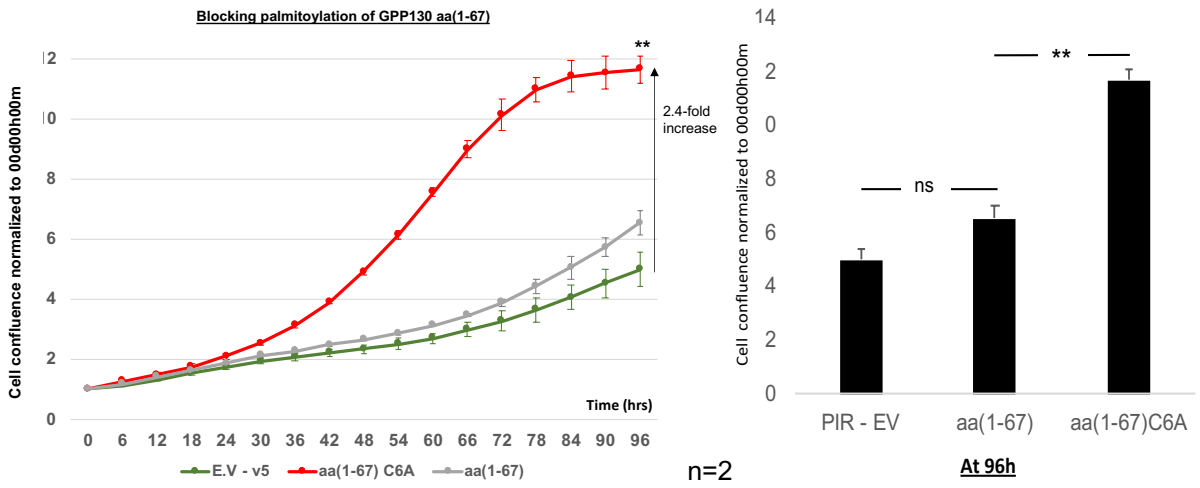

Figure 27: Blocking Palmitoylation of GPP130 NTD promotes growth of A549 Cells

Fig. 27: *(LEFT)* The figure shows the growth curve of A549 lung cancer cells expressing pIRES-V5 EV, GPP130 aa(1-67)-V5 and GPP130 aa(1-67)C6A-V5

(RIGHT) Corresponding bar graph of cell growth at 96 hours. These results are representative of two independent experiments. (ns means p>0.05), (* means p <0.05), (** means p < 0.01) and (*** means p < 0.001) (Student's t test).

Since blocking palmitoylation of GPP130 aa(1-67) showed a significant increase in A549 cell proliferation, we hypothesized a similar result when both palmitoylation and myristoylation are blocked. Thus, we generated a double mutant to prevent both myristoylation and palmitoylation, i.e., GPP130 aa(1-67)G2AC6A and observed its impact on proliferation. Surprisingly, our data showed no difference in A549 cellular growth, and the proliferation was comparable to pIRES-V5 Empty Vector. As both palmitoylation and myristoylation play a significant role in governing the stability of membrane-bound proteins, it is possible that removing both lipid modifications renders the fragment highly unstable, causing its subsequent degradation [62] [63]. Further studies need to be done on the impact of blocking both the lipid modifications, i.e., palmitoylation and myristoylation of the full-length GPP130 protein (GPP130-G2AC6A), on A549 cell proliferation.

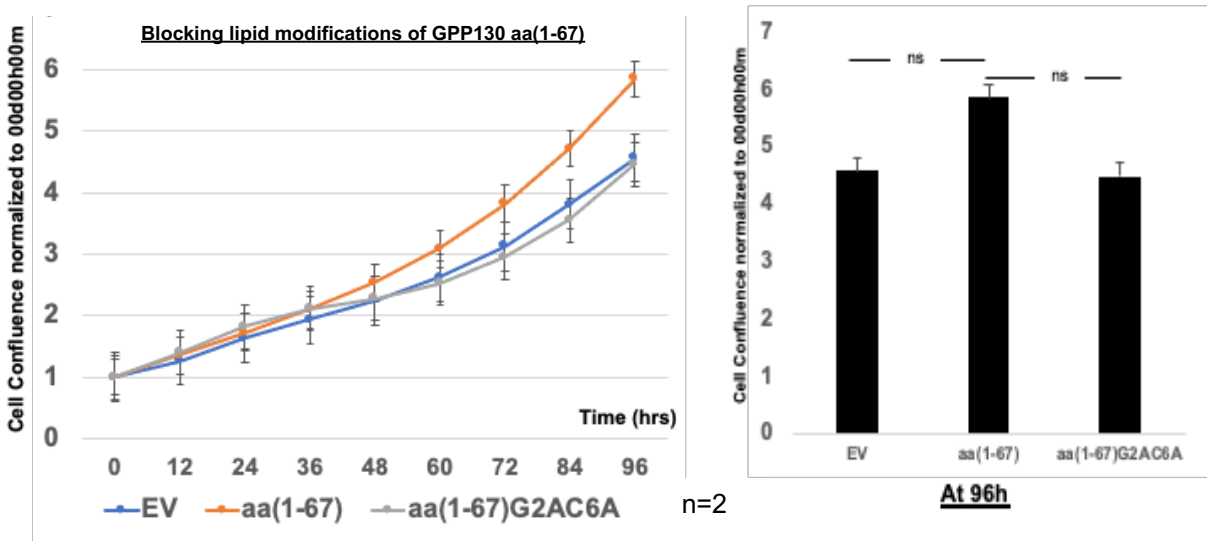

Figure 28: Blocking Lipid Modifications of GPP130 NTD

Fig. 28: *(LEFT)* The figure shows the growth curve of A549 lung cancer cells expressing pIRES-V5 EV, GPP130 aa(1-67)-V5 and GPP130 aa(1-67)G2AC6A-V5

(RIGHT) Corresponding bar graph of cell growth at 96 hours. These results are representative of two independent experiments. (ns means p>0.05), (* means p <0.05), (** means p < 0.01) and (*** means p < 0.001) (Student's t test).

4.13. BOS compounds as a therapeutic strategy

In collaboration with Boston Pharmaceuticals, our laboratory tested potent small molecule inhibitors of proprotein convertases (BOS), especially Furin, manufactured by the company [64]. We used BOS318 to examine if GPP130-induced proliferation can be negatively regulated. To perform this experiment, we first checked the ability of BOS318 to also inhibit PC7 by performing a western blot on cells co-expressing PC7 and transferrin receptor and checking the levels of shed transferrin receptor in media upon treatment of A549 cells with different concentrations of BOS318 (Figure 29). The results show that BOS318 is not a very potent PC7 inhibitor, in contrast to Furin inhibition [64].

However, since BOS318 could block PC7 activity to a certain extent, we decided to investigate if blocking the shedding of GPP130 by PCs (PC7 and Furin) could impact A549 cellular proliferation.

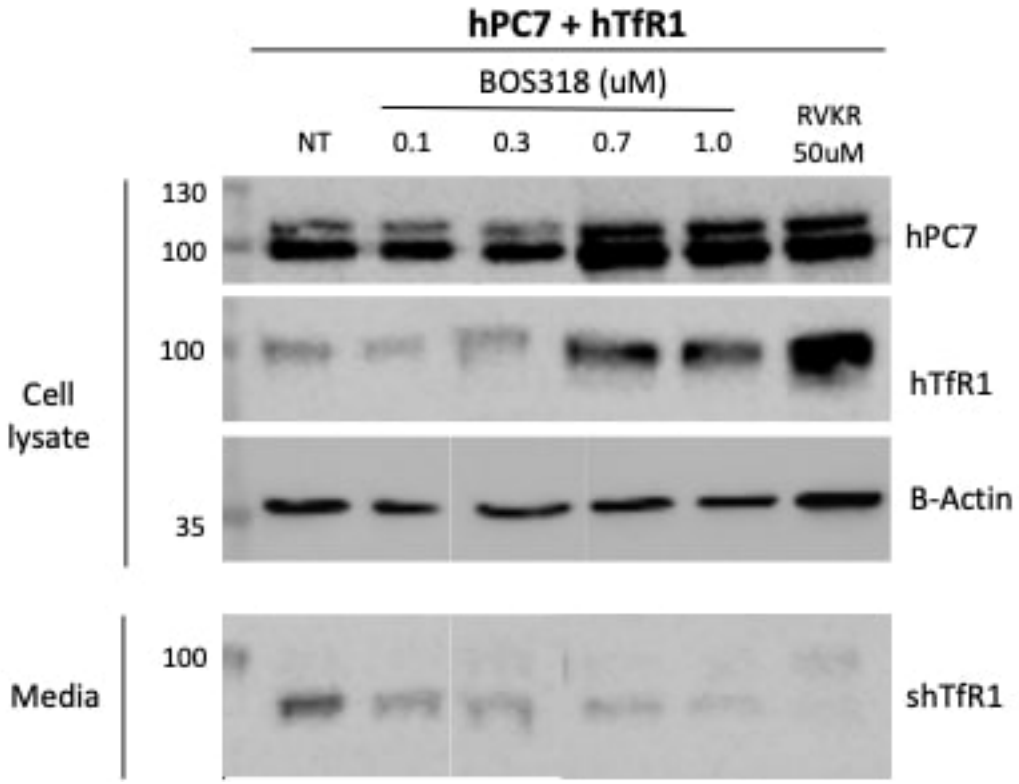

Figure 29: BOS318 blocks PC7 activity on TfR1

Fig. 29: Western blot analysis of cell lysates and media from HEK293 cells overexpressing equimolar quantities of human PC7 and human TfR1, and pIRES-empty vector (Vector) and treated with varying concentrations of BOS318 (0.1, 0.3, 0.7, 1.0 uM) and RVKR (50uM) as a positive control.

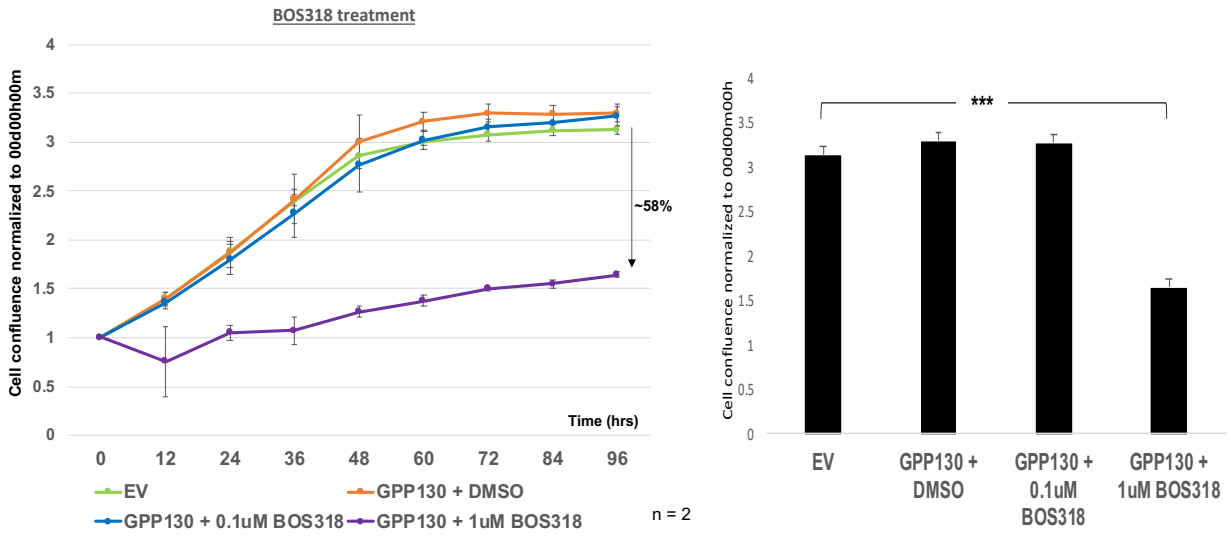

Figure 30: Using BOS318 to block GPP130 induced proliferation in A549 Cells

Fig. 30: *(LEFT)* The figure shows the growth curve of A549 lung cancer cells overexpressing GPP130-v5 and treated with 0.1uM BOS318 and 1.0uM BOS318. (ns means p>0.05), (* means p <0.05), (** means p < 0.01) and (*** means p < 0.001) (Student's t test).

We treated A549 cells with two different concentrations of BOS318 and let the cells grow for 96 hours. Our results show that 1uM BOS318 can vastly reduce proliferation induced by GPP130 in A549 cells (Figure 30). This reduction in proliferation is not necessarily exclusively due to a diminished GPP130-processing but may also reduce the cleavage of other endogenous PC-substrate proteins that regulate A549 cellular proliferation. As mentioned before, BOS318 is a small molecule inhibitor of especially Furin and Furin is implicated in the activation of a multitude of growth factors and their subsequent receptors that play a role in cellular growth. Since 1uM of BOS318 treatment blocks PC7 and Furin, we believe the ~58% reduction in A549 cellular proliferation observed may mainly be due to blocking the activity of these endogenous convertases.

Chapter 5 - Discussion & Future Perspectives

Despite extensive research and the establishment of various targeted therapeutic approaches and/or immunotherapies, survival rates for lung cancer patients remain low. Additionally, it is pivotal for early detection of this cancer to dramatically improve patient prognosis.

Our study presented here aimed to characterize GPP130, a Golgi resident protein that is amplified in ~35% of lung cancer patients.

GPP130 is a protein localized in the Golgi apparatus and follows a distinct pathway for cellular transport. The existing literature primarily focuses on GPP130's involvement in transporting the Shiga toxin within cells [55]. Furthermore, studies aiming to target GPP130 trafficking for therapeutic purposes in the context of Shiga toxin infections have revealed that this protein is responsive to Mn^{2+} and can be redirected for degradation with Mn^{2+} treatments [54]. Previous research has shown that the movement of GPP130 from endosomes to lysosomes is modulated by Sortilin, a well-known sorting protein, and AP-5, a recently identified adaptor protein [59]. These recent investigations suggest that GPP130 can transport various molecules through the secretory pathway and potentially plays a role in rerouting cargo proteins for degradation, although its specific biological functions and cargos have yet to be determined. Notably, a research group studying Ca^{2+} signalling in cancer initiation has emphasized the significance of GPP130 in cell cycle progression and demonstrated that suppressing GPP130 significantly impairs cell proliferation in head-and-neck cancer cells [56].

In this study, we provide evidence for the involvement of GPP130 in the growth of human lung cancer cells. We have shown that overexpression of GPP130 increases the

proliferation of A549 lung cancer cells, and a subsequent knockdown prevents this increase and negatively regulates cell proliferation. Additionally, we reveal that the cleavage of GPP130 by PC7 at **HR**S**R$_{70}$**↓LE generates a soluble fragment, Sol.GPP130-ΔTM that positively impacts cellular proliferation, causing a growth upregulation of A549 cells, suggesting the shedding of GPP130 by PC7 is important in A549 cell growth. We confirm this upregulation by enhanced growth of GPP130-5REL mutants. We further show a media swap experiment, wherein media consisting of Sol.GPP130-ΔTM fragment can upregulate proliferation, suggesting the fragment from the media could bind to a possible receptor, we call it "receptor X", on the surface of A549 cells, potentially initiating a cascade of signalling events that confer cell growth. To further confirm the presence of receptor X, cells could be treated with media containing the Sol.GPP130-ΔTM-V5 fragment and incubated at 4^{o}C overnight. This would prevent the internalization of the fragment after it is bound to the receptor, after which a western blot of cell lysates probed with V5 antibody would support the presence of Receptor X (in progress).

Another future experiment to better understand the molecular mechanisms behind this upregulated proliferation would be to perform RNA Seq of the A549 cells treated with the media containing the ΔTM fragment and compare it with RNA Seq of A549 naïve cells. This would shed light on the differentially regulated mRNAs upon treatment with media having the ΔTM fragment.

We also explored the impact of lipid modifications on the N-terminal Domain of GPP130 aa(1-67) (NTD). Our data showed that blocking S-Palmitoylation at Cys$_6$ (C6A) significantly increases proliferation 2.5-fold over EV, suggesting palmitoylation of GPP130 may have a protective role against tumour progression. This result came as a surprise to us since it is the addition of Palmitic acid to Cysteine residues (S-

Palmitoylation) that functions in the activation of both oncogenes (e.g., EGFR) and tumour suppressors (e.g., SCRIB). In mammalian cells, the process of attaching palmitate to internal cysteine residues is facilitated by a group of enzymes known as DHHC-family palmitoyl S-acyltransferases, consisting of 23 Asp-His-His-Cys enzymes. On the other hand, the removal of palmitate is carried out by serine hydrolases, specifically Acyl-Protein Thioesterases (APTs). These enzymes play a crucial role in regulating the activity of significant oncogenes and tumor suppressors, and their expression patterns often undergo changes in cancer [65].

Since we observed a 2.5-fold increase in proliferation upon blocking S-Palmitoylation of GPP130-NTD, it becomes crucial to see if a similar effect is observed by blocking palmitoylation of GPP130 full-length protein to better understand the role of GPP130 in cancer. To do this, we will generate GPP130-G2A, GPP130-C6A and GPP130-G2AC6A mutations, wherein Gly_2 is modified to Ala_2, Cys_6 is modified to Ala_6.

Additionally, since we identified that Sol-GPP130 ΔTM (aa[71-696]) fragment is responsible for GPP130 induced proliferation of A549 cells, we decided to further narrow down the precise region of GPP130, that upon shedding by PCs incurs a proliferative advantage to cells. Since we already show GPP130 aa(278-696), a fragment generated upon the shedding of GPP130 by Furin at **K**PT**R**$_{277}$↓EV (S2), does not have a proliferative advantage (Figure 21), we believe its GPP130 aa(71-277) is the region of GPP130 that is responsible of GPP130 induced cell proliferation of A549 Cells *(in progress)*.

To further confirm if cleavage of GPP130 by PCs is crucial to enhance proliferation, we propose to generate a GPP130 double mutant to R70A and R277A. This double mutant, GPP130-R70AR277A, should completely prevent the shedding of GPP130 by PC7 and

Furin at S1 and S2, respectively, answering the question if PC activity on GPP130 is pivotal in enhancing cellular proliferation.

To summarize, our study demonstrated, for the first time, that GPP130 undergoes cleavage by PC7 and Furin enzymes. This cleavage process results in the release of an ectodomain fragment, which can potentially hinder cell proliferation. Interestingly, this mechanism bears a resemblance to the behaviour of another protein in the same family, GP73, which also exhibits strong oncogenic properties [66, 67]. This research provides valuable insights into the functions of a Golgi-resident protein that was previously not well understood. Further studies will focus on uncovering its potential biological roles, identifying its binding partners, and examining how the activity of Proprotein Convertases influences its functionality.

REFERENCES

1. Ohkura, H., *Meiosis: an overview of key differences from mitosis.* Cold Spring Harb Perspect Biol, 2015. **7**(5).
2. McIntosh, J.R., *Mitosis.* Cold Spring Harb Perspect Biol, 2016. **8**(9).
3. Schafer, K.A., *The cell cycle: a review.* Vet Pathol, 1998. **35**(6): p. 461-78.
4. Matthews, H.K., C. Bertoli, and R.A.M. de Bruin, *Cell cycle control in cancer.* Nat Rev Mol Cell Biol, 2022. **23**(1): p. 74-88.
5. Wang, Z., *Regulation of Cell Cycle Progression by Growth Factor-Induced Cell Signaling.* Cells, 2021. **10**(12).
6. Musacchio, A. and A. Desai, *A Molecular View of Kinetochore Assembly and Function.* Biology (Basel), 2017. **6**(1).
7. Musacchio, A. and E.D. Salmon, *The spindle-assembly checkpoint in space and time.* Nat Rev Mol Cell Biol, 2007. **8**(5): p. 379-93.
8. Hanahan, D. and R.A. Weinberg, *The hallmarks of cancer.* Cell, 2000. **100**(1): p. 57-70.
9. Collins, K., T. Jacks, and N.P. Pavletich, *The cell cycle and cancer.* Proc Natl Acad Sci U S A, 1997. **94**(7): p. 2776-8.
10. Barrett, J.C. and R.W. Wiseman, *Cellular and molecular mechanisms of multistep carcinogenesis: relevance to carcinogen risk assessment.* Environ Health Perspect, 1987. **76**: p. 65-70.
11. Wojtys, W. and M. Oron, *How Driver Oncogenes Shape and Are Shaped by Alternative Splicing Mechanisms in Tumors.* Cancers (Basel), 2023. **15**(11).
12. Aaronson, S.A., *Growth factors and cancer.* Science, 1991. **254**(5035): p. 1146-53.
13. Moses, H.L., E.Y. Yang, and J.A. Pietenpol, *TGF-beta stimulation and inhibition of cell proliferation: new mechanistic insights.* Cell, 1990. **63**(2): p. 245-7.
14. Fulda, S., *Tumor resistance to apoptosis.* Int J Cancer, 2009. **124**(3): p. 511-5.
15. Shay, J.W. and S. Bacchetti, *A survey of telomerase activity in human cancer.* Eur J Cancer, 1997. **33**(5): p. 787-91.
16. Wittekind, C. and M. Neid, *Cancer invasion and metastasis.* Oncology, 2005. **69 Suppl 1**: p. 14-6.
17. Teng, M.W., et al., *Immune-mediated dormancy: an equilibrium with cancer.* J Leukoc Biol, 2008. **84**(4): p. 988-93.
18. Schwartz, L., C.T. Supuran, and K.O. Alfarouk, *The Warburg Effect and the Hallmarks of Cancer.* Anticancer Agents Med Chem, 2017. **17**(2): p. 164-170.
19. Grivennikov, S.I., F.R. Greten, and M. Karin, *Immunity, inflammation, and cancer.* Cell, 2010. **140**(6): p. 883-99.
20. Esteller, M., *Cancer epigenomics: DNA methylomes and histone-modification maps.* Nat Rev Genet, 2007. **8**(4): p. 286-98.
21. Hanahan, D. and R.A. Weinberg, *Hallmarks of cancer: the next generation.* Cell, 2011. **144**(5): p. 646-74.
22. Hanahan, D., *Hallmarks of Cancer: New Dimensions.* Cancer Discov, 2022. **12**(1): p. 31-46.

23. Whisner, C.M. and C. Athena Aktipis, *The Role of the Microbiome in Cancer Initiation and Progression: How Microbes and Cancer Cells Utilize Excess Energy and Promote One Another's Growth.* Curr Nutr Rep, 2019. **8**(1): p. 42-51.
24. Mithoowani, H. and M. Febbraro, *Non-Small-Cell Lung Cancer in 2022: A Review for General Practitioners in Oncology.* Curr Oncol, 2022. **29**(3): p. 1828-1839.
25. Nasim, F., B.F. Sabath, and G.A. Eapen, *Lung Cancer.* Med Clin North Am, 2019. **103**(3): p. 463-473.
26. Hirsch, F.R., et al., *Lung cancer: current therapies and new targeted treatments.* Lancet, 2017. **389**(10066): p. 299-311.
27. Lemjabbar-Alaoui, H., et al., *Lung cancer: Biology and treatment options.* Biochim Biophys Acta, 2015. **1856**(2): p. 189-210.
28. Collins, L.G., et al., *Lung cancer: diagnosis and management.* Am Fam Physician, 2007. **75**(1): p. 56-63.
29. Rogers, L.D. and C.M. Overall, *Proteolytic post-translational modification of proteins: proteomic tools and methodology.* Mol Cell Proteomics, 2013. **12**(12): p. 3532-42.
30. Uy, R. and F. Wold, *Posttranslational covalent modification of proteins.* Science, 1977. **198**(4320): p. 890-6.
31. Ribet, D. and P. Cossart, *Post-translational modifications in host cells during bacterial infection.* FEBS Lett, 2010. **584**(13): p. 2748-58.
32. Fhu, C.W. and A. Ali, *Protein Lipidation by Palmitoylation and Myristoylation in Cancer.* Front Cell Dev Biol, 2021. **9**: p. 673647.
33. Lopez-Otin, C. and J.S. Bond, *Proteases: multifunctional enzymes in life and disease.* J Biol Chem, 2008. **283**(45): p. 30433-7.
34. Seidah, N.G., et al., *The multifaceted proprotein convertases: their unique, redundant, complementary, and opposite functions.* J Biol Chem, 2013. **288**(30): p. 21473-81.
35. Khatib, A.M., et al., *Proprotein convertases in tumor progression and malignancy: novel targets in cancer therapy.* Am J Pathol, 2002. **160**(6): p. 1921-35.
36. He, Z., A.M. Khatib, and J.W.M. Creemers, *The proprotein convertase furin in cancer: more than an oncogene.* Oncogene, 2022. **41**(9): p. 1252-1262.
37. Seidah, N.G. and A. Prat, *The biology and therapeutic targeting of the proprotein convertases.* Nat Rev Drug Discov, 2012. **11**(5): p. 367-83.
38. Seidah, N.G., A. Pasquato, and U. Andreo, *How Do Enveloped Viruses Exploit the Secretory Proprotein Convertases to Regulate Infectivity and Spread?* Viruses, 2021. **13**(7).
39. Seidah, N.G., et al., *cDNA structure, tissue distribution, and chromosomal localization of rat PC7, a novel mammalian proprotein convertase closest to yeast kexin-like proteinases.* Proc Natl Acad Sci U S A, 1996. **93**(8): p. 3388-93.
40. Durand, L., et al., *The motif EXEXXXL in the cytosolic tail of the secretory human proprotein convertase PC7 regulates its trafficking and cleavage activity.* J Biol Chem, 2020. **295**(7): p. 2068-2083.
41. Guillemot, J., et al., *Implication of the proprotein convertases in iron homeostasis: proprotein convertase 7 sheds human transferrin receptor 1 and furin activates hepcidin.* Hepatology, 2013. **57**(6): p. 2514-24.

42. Ashraf, Y., et al., *Proprotein convertase 7 (PCSK7) reduces apoA-V levels.* FEBS J, 2020. **287**(16): p. 3565-3578.
43. Duval, S., et al., *Shedding of cancer susceptibility candidate 4 by the convertases PC7/furin unravels a novel secretory protein implicated in cancer progression.* Cell Death Dis, 2020. **11**(8): p. 665.
44. Bassi, D.E., et al., *Elevated furin expression in aggressive human head and neck tumors and tumor cell lines.* Mol Carcinog, 2001. **31**(4): p. 224-32.
45. D'Anjou, F., et al., *Molecular Validation of PACE4 as a Target in Prostate Cancer.* Transl Oncol, 2011. **4**(3): p. 157-72.
46. Cheng, M., et al., *Pro-protein convertase gene expression in human breast cancer.* Int J Cancer, 1997. **71**(6): p. 966-71.
47. Mercapide, J., et al., *Inhibition of furin-mediated processing results in suppression of astrocytoma cell growth and invasiveness.* Clin Cancer Res, 2002. **8**(6): p. 1740-6.
48. Page, R.E., et al., *Increased expression of the pro-protein convertase furin predicts decreased survival in ovarian cancer.* Cell Oncol, 2007. **29**(4): p. 289-99.
49. Liu, X., et al., *Loss of E-cadherin and epithelial to mesenchymal transition is not required for cell motility in tissues or for metastasis.* Tissue Barriers, 2014. **2**(4): p. e969112.
50. Bassi, D.E., et al., *Proprotein convertase inhibition results in decreased skin cell proliferation, tumorigenesis, and metastasis.* Neoplasia, 2010. **12**(7): p. 516-26.
51. Sun, X., et al., *Proprotein convertase subtilisin/kexin type 9 deficiency reduces melanoma metastasis in liver.* Neoplasia, 2012. **14**(12): p. 1122-31.
52. Liu, X., et al., *Inhibition of PCSK9 potentiates immune checkpoint therapy for cancer.* Nature, 2020. **588**(7839): p. 693-698.
53. Bachert, C., T.H. Lee, and A.D. Linstedt, *Lumenal endosomal and Golgi-retrieval determinants involved in pH-sensitive targeting of an early Golgi protein.* Mol Biol Cell, 2001. **12**(10): p. 3152-60.
54. Mukhopadhyay, S., et al., *Manganese-induced trafficking and turnover of the cis-Golgi glycoprotein GPP130.* Mol Biol Cell, 2010. **21**(7): p. 1282-92.
55. Mukhopadhyay, S., B. Redler, and A.D. Linstedt, *Shiga toxin-binding site for host cell receptor GPP130 reveals unexpected divergence in toxin-trafficking mechanisms.* Mol Biol Cell, 2013. **24**(15): p. 2311-8.
56. Bai, Y., et al., *Golgi integral membrane protein 4 manipulates cellular proliferation, apoptosis, and cell cycle in human head and neck cancer.* Biosci Rep, 2018. **38**(4).
57. Muhlen, S. and P. Dersch, *Treatment Strategies for Infections With Shiga Toxin-Producing Escherichia coli.* Front Cell Infect Microbiol, 2020. **10**: p. 169.
58. Castro, V.S., et al., *Shiga-toxin Producing Escherichia coli: Pathogenicity, Supershedding, Diagnostic Methods, Occurrence, and Foodborne Outbreaks.* Compr Rev Food Sci Food Saf, 2017. **16**(6): p. 1269-1280.
59. Venkat, S. and A.D. Linstedt, *Manganese-induced trafficking and turnover of GPP130 is mediated by sortilin.* Mol Biol Cell, 2017. **28**(19): p. 2569-2578.
60. Guan, X. and C.A. Fierke, *Understanding Protein Palmitoylation: Biological Significance and Enzymology.* Sci China Chem, 2011. **54**(12): p. 1888-1897.

61. Cadwallader, K.A., et al., *N-terminally myristoylated Ras proteins require palmitoylation or a polybasic domain for plasma membrane localization.* Mol Cell Biol, 1994. **14**(7): p. 4722-30.
62. Linder, M.E. and R.J. Deschenes, *Palmitoylation: policing protein stability and traffic.* Nat Rev Mol Cell Biol, 2007. **8**(1): p. 74-84.
63. Wang, B., et al., *Protein N-myristoylation: functions and mechanisms in control of innate immunity.* Cell Mol Immunol, 2021. **18**(4): p. 878-888.
64. Essalmani, R., et al., *Distinctive Roles of Furin and TMPRSS2 in SARS-CoV-2 Infectivity.* J Virol, 2022. **96**(8): p. e0012822.
65. Ko, P.J. and S.J. Dixon, *Protein palmitoylation and cancer.* EMBO Rep, 2018. **19**(10).
66. Marrero, J.A., et al., *GP73, a resident Golgi glycoprotein, is a novel serum marker for hepatocellular carcinoma.* J Hepatol, 2005. **43**(6): p. 1007-12.
67. Hann, H.W., et al., *Analysis of GP73 in patients with HCC as a function of anti-cancer treatment.* Cancer Biomark, 2010. **7**(6): p. 269-73.